ISSN 0915-6364

NATIONAL INSTITUTE FOR FUSION SCIENCE

Recommended Atomic Data for Collisional-Radiative Model of Li-like Ions and Gain Calculation for Li-like Al Ions in the Recombining Plasma

T. Nishikawa, T. Kawachi, K. Nishihara and T. Fujimoto

(Received - June 26, 1995)

NIFS-DATA-30 Sep. 1995

RESEARCH REPORT
NIFS-DATA Series

NAGOYA, JAPAN

Recommended Atomic Data for Collisional-Radiative Model of Li-like Ions and Gain Calculation for Li-like Al ions in the recombining plasma

T. Nishikawa, T. Kawachi[a], K. Nishihara[b] and T. Fujimoto[c]

Department of Engineering, Okayama University, Okayama, 700, Japan
(a) The institute of Physical and Chemical Research (RIKEN), Saitama, 351-01, Japan
(b) Institute of Laser Engineering, Osaka University, Suita, Osaka, 565, Japan
(c) Department of Engineering Science, Kyoto University, Kyoto, 606, Japan

Abstract

We have assessed atomic data for lithium-like ions for the purpose of constructing a reliable collisional-radiative model. We show several examples of the atomic data for aluminum and oxygen ions, and comparison of data from several sources is done in detail. For ions with nuclear charge z, the scaling formulas and fitting parameters, which are based on the data of oxygen ions, are presented. By use of these data, we have constructed two collisional-radiative models: the one for aluminum ions and the one for ions according to the scaling for z. The population inversion and the amplification gain of the soft x-ray laser lines in the recombining aluminum plasma are calculated for several electron temperatures. We also examine the effects of ion collisions for Δn=0 transitions on the excited level populations.

Keywords: lithiumlike ions, recombining plasma, soft x-ray laser

I. THE FORMULATION OF COLLISIONAL-RADIATIVE (CR) MODEL (FINE STRUCTURE UNRESOLVED)

The population density of the ground and excited levels of ions in plasma is determined by various collisional and radiative atomic processes taking place in the plasma. For level p, the temporal development of its population $n(p)$ is expressed by the differential equation,

$$\begin{aligned}\frac{dn(p)}{dt} &= \sum_{q<p} C(q,p) n_e n(q) \\ &- \{[\sum_{q<p} F(p,q) + \sum_{q>p} C(p,q)] n_e + \sum_{q<p} A(p,q)\} n(p) \\ &+ \sum_{q>p} [F(q,p) n_e + A(q,p)] n(q) - S(p) n_e n(p) \\ &+ [\alpha(p) n_e + \beta(p) + \gamma(p)] n_e n_{He} \end{aligned} \quad (1)$$

which is coupled with similar equations for other levels. Here "$q < p$" means that level q lies energetically lower than level p. $A(p,q)$ is the spontaneous transition probability from p to q, and $C(p,q)$, $F(q,p)$ and $S(p)$ are the rate coefficients for electron impact excitation, deexcitation, and ionization, respectively, and $\alpha(p)$, $\beta(p)$ and $\gamma(p)$ are the rate coefficients for three-body, radiative and dielectronic recombination, respectively. n_e is electron density, and we express the ground state helium-like ion density as n_{He}. According to the method of the quasi steady state solution, the time derivative of the population of excited levels is assumed equal to 0, so that the set of coupled differential equations for excited levels reduces to a set of coupled linear equations. The solution is expressed as the sum of the two terms;

$$n(p) = R_0(p) n_e n_{He} + R_1(p) n_e n_{Li} \quad (2)$$

where $R_0(p)$ and $R_1(p)$ are the population coefficients which are determined by the actual collisional and radiative processes and are functions of n_e and electron temperature T_e. The ground state Li-like ion density *i.e.*, $n(2^2S)$, has been expressed as n_{Li}. The first term may be called the recombining plasma component and the second term is the ionizing plasma component [1].

In the case of a CR model with fine structure unresolved, we assume that the fine structure sublevels belonging to a level are populated according to their statistical weights. Let p in eq.(1) represent the principal quantum number n and the azimuthal quantum number l, and $n(p)$ is the sum of the populations of the fine structure sublevels. Each of the rate coefficients in eq.(1) refers to level p or q, and is related to the rate coefficients for transitions connecting

individual fine structure sublevels; *i.e.*, it is the average over the initial fine structure sublevels and the sum over the final sublevels.

$$B(p,q)=\frac{g(p_1)}{g(p)}\{B(p_1,q_1)+B(p_1,q_2)\}+\frac{g(p_2)}{g(p)}\{B(p_2,q_1)+B(p_2,q_2)\} \tag{3}$$

where $B(p,q)$ stands for $C(p,q)$, $A(p,q)$ or $F(p,q)$ and p and q denote the initial and final levels, respectively. Here p_1 and p_2 mean the fine structure sublevels with total angular momentum $j = l-1/2$ and $j = l+1/2$, respectively, and $g(p)$ is the statistical weight of level p. In the case of an S state, p_1 or q_1 term is absent. The ionization rate coefficient is defined as

$$S(p)=\frac{g(p_1)}{g(p)}S(p_1)+\frac{g(p_2)}{g(p)}S(p_2) \tag{4 a}$$

and the recombination rate coefficient is defined as

$$\alpha(p)=\alpha(p_1)+\alpha(p_2) \tag{4 b}$$

for $\alpha(p)$ and similarly for $\beta(p)$ or $\gamma(p)$.

II. ATOMIC DATA FOR Li-LIKE IONS FOR VARIOUS Z

A) Energy Levels

The energy levels of the ground states and low-lying excited levels of Li-like ions are calculated by Lindgard and Nielsen [2], and Sureau *et al.* [3] with neglect of fine structure, and Zhang *et al.* [4] for fine structure levels.

All of the data, with eq. (3), agree well. The ionization potentials of the ground state for various z ions are expressed as

$$E\ (2s) = 2.60910\times(z\ -2) + 3.39323\times(z\ -2)^2 + 1.94126\times10^{-3}\times(z\ -2)^3\ \text{(eV)}$$
$$\text{for}\ z\ : 6 \le z\ \le 50 \tag{5}$$

and the transition energy from the ground state to the levels with $n \le 5$ are fitted by the polynomial formula defined as,

$$E\ (n\ l\ ) = \sum_{k=1}^{4} C_{k} \times (z-2)^{k} \quad \text{(eV)} \tag{6}$$

The fitting parameters C_k's are listed in TABLE II-1. The error of the fitting formula is within 1% for $6 \le z \le 40$.

The energy level for the $n \ge 6$ levels, we assum the hydrogenic approximation, *i.e.*, the level energy measured from the ionization limit is given as

$$E = \frac{(z-2)^2\,\mathrm{Ry}}{n^2} \quad \text{(eV)} \tag{7}$$

where R_y is one Rydberg.

B) Absorption oscillator strength

B-1. $\Delta n \neq 0$ transitions

The absorption oscillator strength is given by Lindgard and Nielsen [2], Zhang *et al.* [4] and the compilation by Wiese. [5]

The absorption oscillator strength among the levels with $n \le 5$ for the ion z is expressed by

$$f\ (i,\ f) = C_1 + \frac{C_2}{(z-2)^2} + C_3 \times \exp\left(-C_4 \times (z-2)^{0.4}\right) \tag{8}$$

and the fitting parameters C_k's are listed in TABLE II-2. For transitions from level with $n \le 4$ to upper levels with $6 \le n \le 10$,

$$f\ (nl\ ,n'l')_z = f\ (nl\ ,5l')_z \times \left(\frac{n}{5}\right)^{a}$$
$$\text{for } n \le 4,\ 6 \le n' \le 10 \tag{9}$$

these fitting parameters a are listed in TABLE II-3. For the transitions from the $n = 5$ levels to upper levels with $6 \le n \le 10$,

$$f\ (5s, n\ ) = 0.608 \times (n/6)^{-3}$$
$$f\ (5p, n\ ) = 0.700 \times (n/6)^{-3}$$
$$f\ (5p, n\ ) = 0.700 \times (n/6)^{-3}$$
$$f\ (5f, n\ ) = 1.208 \times (n/6)^{-3}$$
$$f\ (5g, n\ ) = 1.683 \times (n/6)^{-3} \tag{10}$$

and in the case of $n \geq 11$,

$$f\ (nl, n'l')_Z = f\ (nl, 10'l')_Z \times \left(\frac{n}{10}\right)^{-3}$$
$$\text{for } n' \geq 11 \qquad (11)$$

For transitions among the $n \geq 6$ levels, we assume the hydrogenic approximation.

B-2. Δn=0 (l-changing) transition
The oscillator strength of $2s\ ^2S_{1/2}$-$2p\ ^2P_{1/2,\ 3/2}$ is given by

$$f\ (2s\ ^2S_{1/2}\text{–}2p\ ^2P_{1/2}) = 0.82900 + \frac{1.3392}{(z-2)^2} - 0.77803 \times \exp\left(1.2187\times10^{-2} \times (z-2)^{0.4}\right)$$
$$f\ (2s\ ^2S_{1/2}\text{–}2p\ ^2P_{3/2}) = 8.8928 \times 10^{-2} + \frac{2.4051}{(z-2)^2} - 3.4939 \times 10^{-3}\ (z-2) - 6.6531 \times 10^{-5}\ (z-2)^2$$

and for other transitions, the oscillator strength is expreesed as

$$f\ (nl, n\ l')_Z = C_1 \times \left(\frac{8-2}{z-2}\right) \qquad (12)$$

where the parameter C_1 is the absorption oscillator strength for oxygen. (See TABLE II-4.)

C) Electron impact excitation cross sections and rate coefficients

C-1. Cross sections
$\Delta n \neq 0$ transitions

For transitions $2s\ ^2S_{1/2}$-$2p\ ^2P_{1/2,3/2}$, $2s\ ^2S_{1/2}$-$3p\ ^2P_{1/2,3/2}$ and $2s\ ^2S_{1/2}$-$3s\ ^2S_{1/2}$, there are many theoretical, experimental and semi-empirical cross section data [4,6-11]. Comprehensive data for oxygen to uranium are given by Zhang *et al.* [4] who treat the fine structure sublevels separately. For Li-like oxygen ions, virtually all the transitions among the levels from $2s\ ^2S$ to $5g\ ^2G$ are calculated by Clark, Abdallah and Csanak. (C,A,C), and details of the calculation method is given in [12].

For optically allowed transitions, the results by Zhang *et al.* [4] and C,A,C are in good agreement. In the high energy range, the hydrogenic approximation by Clark *et al.* [11] for 2^2S-3^2P is larger by a factor 1.5 than the result by Zhang *et al.* and for 2^2P-3^2S, smaller by a factor 2.5. These differences may be attributed to the oscillator strength values of hydrogenic 2^2S-3^2P and 2^2P-3^2S transitions which are larger and smaller than those of OVI approximately by those amounts, respectively. (See the following Section.)

The cross sections for the transitions from the ground state and the first excited levels are referred to ref.[4], and for other transitions among the levels with $n \leq 5$ levels calculation by C,A,C [13] is adapted. The fitting formula are expressed as

$$\sigma_{\text{oxygen}}(i, f) = \pi a_0^2 [A \frac{\log E}{E} + \frac{B}{E} + C \times \exp(-DE)] \tag{13}$$

The parameters for these transitions and 2^2S-2^2P are listed in TABLE II-5.

The cross sections for transitions from the level with $n \leq 4$ to those with $n \geq 6$ are scaled as

$$\sigma(E/E_{th})_{n\,l \to n'\,l'} = \sigma(E/E_{th})_{n\,l \to 5\,l'} \times (\frac{f(nl, n'l')}{f(nl, 5l')})$$
$$\text{for } n \leq 4,\ 6 \leq n' \leq 10 \tag{14}$$

where f_{if} is the absorption oscillator strength for the transition from i to f.

For other Li-like ions with nuclear charge z, we recommend Zhang's cross section data for the transitions from the ground state and from $2p\ ^2P_{1/2,3/2}$. For other transitions among the $n \leq 5$ levels, we assume the following scaling formula (optically allowed transitions),

$$\sigma(E/E_{th}) = \sigma_{\text{oxygen}}(E/E_{th}) (\frac{Z-s}{8-s})^{-4} \frac{f_z}{f_{\text{oxygen}}} \tag{15}$$

where σ_{oxygen} is the cross section for OVI ions expressed in the threshold units, s is the screening constant given by Mayer [13] for the lower level, and f_z is the absorption oscillator strength for ion z.

For optically forbidden transitions of oxygen, all the cross sections available agree well. For other z ions, we scale the data by Zhang *et al.* and by C,A,C in the similar way to the optically allowed transition,

$$\sigma(E/E_{th}) = \sigma_{\text{oxygen}}(E/E_{th}) (\frac{Z-s}{8-s})^{-4} \tag{16}$$

Δn=0 transition

For transitions of 3s ^2S-3p $^2P_{1/2,3/2}$, 3p $^2P_{1/2,3/2}$-3d $^2D_{3/2,5/2}$, 4^2S-4^2P, 5^2S-5^2P, there are theoretical calculations [14,15]. We adopt the formula (13) and show the fitting parameters in TABLE II-6.

For other transitions, we use the formulation by Dickinson-Fujima [16,17] which is expressed as

$$\sigma(n,l\text{-}n,l\text{+}1)=6\pi a_0^2[1/(z\text{-}2)^2]\times n^4\times(v_a/v)^2\times(l\text{+}1)/(2l\text{+}1)\times\ln[0.5\times(E/E_{th})] \qquad (17)$$

where v_a is the classical velocity of the orbital electron in the initial level and the v is the velocity of the colliding electron.

C-2. Deexcitation Rate coefficients

$\Delta n \neq 0$ transition

The deexcitation rate coefficients for the Li-like oxygen ions are fitted by the formula

$$F(i,f)_{\text{oxygen}} = [\mathrm{K}\times\frac{\log(T_e)}{T_e^{\mathrm{L}}} + \frac{\mathrm{M}}{T_e} + \mathrm{N}\times\exp(-\mathrm{P}\times T_e)]\times\mathrm{Q} \quad (T_e \text{ in eV}) \qquad (18)$$

The parameters are listed in TABLE II-7.

The deexcitation rate coefficient is related with the excitaion rate coefficient by the principle of detail balance.

For transitions between the excited levels whose principal quantum number is $n \geq 6$, we recommend the semi-empirical cross sections and excitation rate coefficients by Vriens and Smeets [18].

$\Delta n=0$ transition

The scaling equation for other z ion is referred to eq. (18) The fitting parameters for the Li-like oxygen ions are shown in TABLE II-8.

D) Ionization cross sections and rate coefficients

Collision strength and rate coefficients for electron impact ionization process are presented by Sampson and co-workers [19-24], which agree with the calculation by Kunc [25] and semi-empirical formula cross section by Lotz [26]. Fitting parameters of these data are also presented in [19-24]. For $n \geq 6$ levels, we recommend hydrogenic cross section by Vriens and Smeets [18].

E) Radiative recombination

Burgess [27] gives the radiative recombination rate coefficient for hydrogenic ions. MacLaughlin and Hahn [28] modify the result to non-hydrogenic case. In the case of Li-like ions, free-bound oscilaltor strength of each level is rather close to that of hydrogenic ions. We recommend the data by Burgess for Li-like ions.

F) Dielectronic recombination

Dielectronic recombination is an important process in high temperature regions. This process consists of two processes; electron capture into a doubly excited level (dielectronic capture), and a radiative decay which competes with autoionization. The electron capture rate coefficient r_d is associated with the autoionization probability A_a through the detailed balance,

$$[n_{He} n_e r_d(p, nl) = n_{Li}(p, nl) A_a]_E \tag{19}$$

where $n_{Li}(p,nl)$ is the density of the doubly excited Li-like ions. Here $[\ ]_E$ means that this equality holds in thermodynamic equilibrium; *i.e.*, these densities are given by the Saha-Boltzmann relationship. Dielectronic recombination rate coefficient is given by,

$$\gamma(nl) = \sum_p r_d(p, nl) \frac{A_r}{A_r + A_a} \tag{20}$$

where A_r is the radiative decay probability. We consider $2pnl$ and $3pnl$ ($n \geq 2$) levels as the doubly excited levels, and we use the autoionization probability and radiative decay probability given by Bely and Dubau [29] for the OVI ion. For other z elements, we estimate the autoionization probability and the radiative decay probability by a scaling in which relativistic effects are included [30] from those of OVI. (See TABLE II-9)

III. ATOMIC DATA FOR Li-LIKE ALUMINUM IONS

In this section, the atomic data are restricted to Li-like Aluminum ions. Validity of the fitting formula described in section II is examined.

A) Energy Level

The data of energy level published in literature are based on theoretical calculations and spectroscopy. We pick up four different data sources to establish a reliable set of energy levels of Li-like Al ions. Summary of each data source are as follows.

A. Lindgard and S. E. Nielsen [2]

a) The atomic states are identified by n (principal quantum number) and l (azimuthal quantum number).

b) Calculated and evaluated by careful comparison with data for other Li-like ions.
c) Values are given up to n=12.

H. L. Zhang, D. H. Sampson and C. J. Fontes [4]
a) The atomic states are identified by n, l and j (total angular momentum quantum number).
b) Calculated based upon the DFS (Dirac-Fock-Slater) wave function.
c) Values are given for $n \leq 5$.

D. Duston and J. Davis [31]
a) The atomic states are identified by n and l.
b) The values are used to construct atomic model of aluminum plasma in the 1980's.
c) Values are given for $n \leq 5$.

R. L. Kelly [32]
a) The atomic states are identified by n, l and j.
b) Based on spectroscopy.
c) Values are given for many levels including highly excited ones. No data are available for levels which cannot be observed by spectroscopy even for levels with the principal quantum number of 3.

The principle of the evaluation procedure is
a) The data from spectroscopy is regarded most reliable: Kelly's value is adopted when it is available.
b) The n-dependence of the differences in level energy between the different-l levels of a same principal quantum number is derived by Lindgard's calculation.
c) The data of the other two sources are almost the same as Kelly's results: They are used for cross-check.

The evaluated energy level of Li-like Al are shown in TABLE III-1 as compared to four mentioned cases of energy above.

The result of the fitting formula described in section II is shown in the last column of TABLE III-1. All the values given by the fitting formulas are accurate within 1%.

B) Oscillator strength

Almost all the data of oscillator strength published in literature are based on theoretical calculations. We pick up a Guennou's calculation [3] besides the above-mentioned two data

sources, i.e., Lindgard [2] and Zhang *et al.* [4], to establish a set of reliable oscillator strengths. Summary of Guennou's data is

H. Guennou and A. Sureau [3]

a) The atomic states are identified by n, l and j.

b) Theoretical calculations based upon the HF (Hartree-Fock) approximation.

c) Values for transitions between the $n<5$, $n'<7$ ($n \neq n'$) are given.

In the evaluating procedure we took the ratio of the Li-like Al oscillator strength to the hydrogenic value of the corresponding transition as a parameter for comparison. TABLE III-2 shows the ratio in the fifth column. The ratio against n is found to monotonously vary and converge to a value near unity. In the case of d-f, and f-g transitions, the ratio is unity for all the cases.

Some of the ratios based on Lindgard's result are not monotonous functions, and we fixed the value to make the ratio to be a monotonous function. The value of Zhang's and Guennou's are referred to for cross-check.

Table III-2 gives the evaluated oscillator strengths together with the original values from the three sources. Almost all the values by the fitting formula agree within a few percents.

C) Electron impact ionization

The cross section and/or the rate coefficient have already been discussed in Section II.

D) Electron impact excitation

We use the following four fitting formulas to the cross section for electron impact excitation process. Throughout this subsection, a factor of 1/2 (=1/(2S+1)) of the statistical weight is absent in the expressions of cross sections and rate coefficients, which is included in the fitting parameters.

D-1. transitions from n=2

H. L. Zhang, D. H. Sampson and C. J. Fontes [4]

In ref. [4], cross section for Li-like ions is calculated by the distorted wave method. Collision strength at six different colliding energies of the electron is given. For convenience, we fit the cross section by the following formula.

$$Q_{ij} = \frac{\pi a_0^{\,2}}{(2l+1)E_{\mathrm{Ry}}}\Omega_{ij}$$

$$\Omega_{ij} = A_{ij}\ln(\varepsilon) + D_{ij} + \frac{c_1(ij)}{[a_{ij}+\varepsilon]} + \frac{c_2(ij)}{[a_{ij}+\varepsilon]^2} + \frac{c_3(ij)}{[a_{ij}+\varepsilon]^3}$$

$$\varepsilon = \frac{E}{E_{\mathrm{th}}}$$

where Ω_{ij} is the collision strength and E_{th} is the threshold energy of excitation. The six parameters are adjusted so as to give the best fit. These parameter values for each transition are given in TABLE III-3. The excitation rate coefficient is

$$C_{ij} = \pi a_0^{\,2} \left(\frac{8kT}{\pi m}\right)^{1/2} \frac{1}{(2l+1)} \frac{I_H}{kT} \left\langle \Omega_{ij} \right\rangle_{\text{Maxwellian}}$$

$$\left\langle \Omega_{ij} \right\rangle_{\text{Maxwellian}} = D_{ij}\, e^{-y} + A_{ij}\, E_1(y) + y\, e^{a_{ij} y}$$

$$\left[c_1(ij)\, E_1(a_{ij} y + y) + \frac{c_2(ij)}{a_{ij}+1} E_2(a_{ij} y + y) + \frac{c_3(ij)}{[a_{ij}+1]^2} E_3(a_{ij} y + y) \right]$$

$$y = \frac{T}{E_{th}}$$

where E_1, E_2 and E_3 are the exponential integrals.

D-2, Transitions from n=3-4 to n=4-5

L.B. Golden, R. E. H. Clark, S. J. Goett and D. H. Sampson [33]

R. E. H. Clark, D. H. Sampson and S. J. Goett [11]

In refs. [11] and [33], cross sections are given in the hydrogenic approximation. We modified these cross sections on the basis of the following argument. Fig. III-1 shows the cross section for transitions 2^2S-3^2S, -3^2P and -3^2D. Fig. III-1 (a) shows the cross sections in the hydrogenic approximation and Fig. III-1 (b) shows those of Li-like Al as described in the previous subsection D-1. This figure suggests the former approximation agree with the latter for the dipole forbidden transitions 2^2S-3^2S and 2^2S-3^2D. A substantial difference is seen in the case of dipole allowed transition 2^2S-3^2P. Therefore we multiply the hydrogenic cross section by the ratio of the oscillator strength of Li-like to that of hydrogenic ions for the dipole allowed tramsition. In the present case of 2^2S-3^2P transition, the ratio is 0.77.

The fitting formula is shown in ref [33] and [11]. The cross section of the Li-like Al ion is given by

$$Q_{ij} = \frac{\pi a_0^{\,2}}{(2l+1)} \frac{1}{E_{Ry}} \Omega_{ij} \left(\frac{\text{Oscillator strength of Li-like Al}}{\text{Oscillator strength of H-like}} \right)_{\text{if dipole allowed}}$$

$$Z^2 \Omega_{ij} = A_{ij} \ln(\varepsilon) + D_{ij} + \frac{c_1(ij)}{[a_{ij}+\varepsilon]} + \frac{c_2(ij)}{[a_{ij}+\varepsilon]^2}$$

$$\varepsilon = \frac{E}{E_{th}}$$

where Z_{eff} is the screened charge and is equal to Z -s in eq. (15) or (16), a_0 is the Bohr radius.

The parameters are given for each transition in TABLE III-4. The excitation rate coefficient is given by

$$C_{ij} = \pi a_0^{\,2} \left(\frac{8kT}{\pi m}\right)^{1/2} \frac{1}{(2l+1)} \frac{I_H}{kT} \frac{1}{Z_{eff}^{\,2}} \left\langle Z^2 \Omega_{ij} \right\rangle_{\text{Maxwellian}}$$

$$\left\langle Z^2_{\text{eff}} \Omega_{ij} \right\rangle_{\text{Maxwellian}} = D_{ij}\, e^{-y} + A_{ij}\, E_1(y) + y\, e^{a_{ij} y}$$

$$\left[c_1(ij)\, E_1(a_{ij}\, y + y) + \frac{c_2(ij)}{a_{ij}+1}\, E_2(a_{ij}\, y + y) + \right] \left(\frac{\text{Oscillator strength of Li-like Al}}{\text{Oscillator strength of H-like}}\right)_{\text{if dipole allowed}}$$

$$y = \frac{T}{E_{th}}$$

c) Others ($n \neq n'$)

D. H. Sampson and H. L. Zhang [34]

In ref [34], cross section in the hydrogenic approximation is given. We derive the cross section based on this approximation.

We adopt the fitting formula in [34].

$$Q_H = \frac{\pi a_0^{\,2}}{n^2} \frac{1}{E_{Ry}} \frac{Z^2}{Z_{eff}^{\,2}} \Omega_{ij} \left(\frac{\text{Oscillator strength of Li-like Al}}{\text{Oscillator strength of H-like}}\right)_{\text{if dipole allowed}}$$

$$Z^2 \Omega_H = A_{ij} \ln(\varepsilon) + D_{ij} \left(1 - \frac{1}{\varepsilon}\right) + \frac{c(ij)}{\varepsilon}$$

$$\varepsilon = \frac{E}{E_{th}}$$

The parameters for each transition are given in TABLE III-5. The excitation rate coefficient is given by

$$C_{ij} = \pi a_0^{\,2} \left(\frac{8kT}{\pi m}\right)^{1/2} \frac{1}{n^2} \frac{I_H}{kT} \frac{1}{Z_{eff}^{\,2}} \left\langle Z^2 \Omega_{ij} \right\rangle_{\text{Maxwellian}}$$

$$\left\langle Z^2_{\text{eff}} \Omega_{ij} \right\rangle_{\text{Maxwellian}} = (A_{ij} + y\, c_{nn'})\, E_1(y) + D_{ij}\, E_2(y)$$

$$\left(\frac{\text{Oscillator strength of Li-like Al}}{\text{Oscillator strength of H-like}}\right)_{\text{if dipole allowed}}$$

$$y = \frac{T}{E_{th}}$$

d) l-changing collisions ($n=n'$)

We adopt Seaton's formula (Bethe approximation).

$$C_{kk'} = 1.58 \times 10^{-5}\ T\ (\mathrm{eV})^{-3/2}\ \frac{1}{y}\ f_{kk'} \exp(-y) \quad (\mathrm{cm}^3/\mathrm{s})$$
$$y = \frac{T}{E_{\mathrm{th}}}$$

where $f_{kk'}$ is the oscillator strength, and T (eV) is the electron temperature in the eV units.

E) Radiative Recombination

We adopt the formula for hydrogenic ions.

$$C_{nl} = 5.20 \times 10^{-14}\ Z_n\ y^{-1.5} \exp(y)\ E_1(y)\ \frac{g_{nl}}{g_n} \quad (\mathrm{cm}^3/\mathrm{s})$$
$$y = \frac{T}{E_{\mathrm{th}}}$$

where g_{nl} and g_n are the statistical weight of the level nl and the levels with the principal quantum number n, respectively. This is equivalent to assuming that the free-bound Gaunt factor is 1.

IV. POPULATION DISTRIBUTION AND RESULTANT GAIN IN THE RECOMBINING Li-LIKE Al PLASMA

Population density is calculated in the quasi-steady state approximation and neglecting the ionizing plasma component which is described in Section I. We show typical three cases of T_e=20eV, 30eV and 50eV, which correspond to the experiments. [35,36] Resultant gain in the recombining plasma is also shown. The line profile is assumed to be simple Doppler broadening.

A) Case using the atomic data described in Section III.

Fig. IV-1, Fig IV-2, and Fig. IV-3 show the calculated result for population and amplification gain for T_e=20, 30 and 50eV, respectively. In all the case, the gain of the transitions to the 3^2P state is always negative though positive gain is observed in experiment. [35] It is noted that the result is very sensitive to the magnitude of the rate coefficients for l-changing collisions in the shell of a same principal quantum number. Fig. IV-4 and 5 show the amplification gain for T_e=30 and 50eV, respectively, without the l-changing process (a), and with the l-changing process (b). For the l-changing process, ion collisions may be more effective than the electron collisions as assumed here. This process will be discussed in the following subsection. The gain of the transition of 3^2D-5^2F is much lower than that of 3^2D-4^2F. The experimental result [36] shows that the gains of 3^2D-5^2F, 3^2P-5^2D, 3^2D-4^2F and 3^2P-4^2D are comparable in magnitude. In the case of recombining plasma of such low temperatures, the population densities of the 5^2D and 5^2F levels are determined by collisional processes resulting in the population density approximately given by local thermodynamic equilibrium (LTE). The population density of the 3^2D level is determined by collisional deexcitation from higher levels and radiative decay to the 2^2P level. Therefore, the estimate of the population densities and the gain is quite insensitive to a small change of the rate coefficients. The oscillator strength of 3^2D-5^2F transition is about 6.5 times smaller than that of 3^2D-4^2F. Therefore, it is difficult to bring the gain of 3^2D-5^2F to a similar magnitude to that of 3^2D-4^2F within the framework of the collisional-radiative recombining plasma.

In the case of T_e=20eV the gain maximum of the 3^2D-4^2F transition appears at around n_e=2×10^{19}cm^{-3} and that of the 3^2D-5^2F transition appears at around n_e=6-8×10^{18}cm^{-3}.

B) Case using the atomic data described in Section II (including ion impact l-changing processes)

Fig. IV-6, Fig IV-7, and Fig. IV-8 show the calculated result for population and amplification gains for T_e=20, 30 and 50eV, respectively. Ion impact l-changing processes are included. Cross section of these processes are derived for the data in Table II-6 and eq.(17) by use of the velocity scaling. We assume the ion density to be 10% of the electron density. In this case, the gains of the transitions to the 3^2P level, *i.e.*, 3^2P-4^2D and 3^2P-5^2D, have positive values. The gain ratio of the transition of 3^2P-4^2D to that of 3^2D-4^2F is consistent with the experimental result. From the comparison with the former case, it is concluded that the l-changing processes by ion collisions are essential for treating these high density plasmas. For the transitions from n=5 levels to n=3, the calculated result is in seriously disagreement with the experimental result, *i.e.*, the calculated gains are smaller than those of the experiment by 2 orders in consistent with A).

For T_e=20eV, gain maximum appears around $n_e=2\times10^{19}$cm^{-3} for the 3^2D-4^2F transition and $n_e=8\times10^{18}$cm^{-3} for the 3^2D-5^2F transition.

Acknowledgement

This work was carried out under the collaborating research program at the National Institute for Fusion Science.

References

[1] T. Fujimoto, J. Phys. Soc. Jpn. **47**, 265 (1979)

[2] A. Lindgard and S.E. Nielsen, Atomic data and Nuclear data table **19**, 533 (1977)

[3] H. Guennou and A. Sureau, J. Phys. B**20**, 919 (1987)

[4] H.L. Zhang, D.H. Sampson and C.J. Fontes, Atomic data and Nuclear data table **44**, 31 (1990)

[5] W.L. Wiese, M.W. Smith and B.M. Glennon, NSRDS-NBS 4 (1966)

[6] C.M. Varsavski, Planet. Space Sci **11**, 1001 (1963)

[7] J.B. Mann, IPPJ-AM-**27**, Inst.Plasma Phys.,Nagoya Univ., Nagoya, (1983)

[8] R. Mewe, Astron & Astrophys. **20**, 215 (1972)

[9] R.E.H. Clark, A.L. Merts, J.B. Mann and L.A. Collins, Phys. Rev. A**27**, 1812 (1983)

[10] K. Bhadra and R.J.W. Henry, Phys. Rev.A**26**, 1848 (1982)

[11] R.E.H. Clark, D.H. Sampson and S.J. Goett, Astrophys. J Spl **49**, 545 (1982)

[12] R.E.H.Clark, G. Csanak and J. Abdallah,Jr., Phys.Rev. A**44**, 2935 (1991)

[13] H. Mayer, Los Alamos Scientific Laboratory Report No LA-607 (1947)

[14] D.H. Sampson and A.D. Parks, Astrophys. J. Supl.263,**28**, 323 (1974)

[15] V.L.Jacobs and J.Davis, Phys.Rev.A**18**,697(1978)

[16] A.S. Dickinson, Astron.Astrophys. **100**, 302 (1981)
[17] K. Fujima Private communication
[18] L. Vriens and A.H.M. Smeets Phys. Rev A**22**,940 (1980)
[19] L.B. Golden and D.H. Sampson J. Phys. B**10**,2229 (1977)
[20] L.B. Golden, D.H. Sampson and K. Omidvar, J. Phys. B**11**, 3235 (1978)
[21] D.L. Moore, L.B. Golden and D.H. Sampson, J. Phys. B**13**, 385 (1980)
[22] D.H. Sampson and L.B. Golden, J. Phys. B**12**, L785 (1979)
[23] L.B. Golden and D.H. Sampson, J. Phys. B**13**, 2645 (1980)
[24] R.E.H. Clark and D.H. Sampson, J. Phys. B**17**, 3311 (1984)
[25] J.A. Kunc, J. Phys. B**13**, 587 (1980)
[26] W. Lotz, Astrphys.J.Suppl. **14**, 207 (1967)
[27] A. Burgess, Mem. Roy. Astr. Soc. **69**, 1 (1964)
[28] D.J. MacLaughlin and Y. Hahn, Phys. Rev. A**43**, 1313 (1991)
(Errata; Phys. Rev. A**45**, 5317 (1992))
[29] F. Bely-Dubau, J. Dubau, P. Faucher and L. Steenman-Clark,
J. Phys. B**14**, 3313 (1981)
[30] L.A. Vainstein and U.I. Safronova, Atomic data and Nuclear data table **34**, 17 (1984)
[31] D. Duston and J. Davis, Phys. Rev. A **23**, 2602
[32] R. L. Kelly, J. Phys. and Chem. Ref. Data **16**, Suppl. 1 (1987)
[33] L. B. Golden, R. E. H. Clark, S. J. Goett and D. H. Sanpson, Astrophys. J. Suppl. **45**, 603 (1981)
[34] D. H. Sampson and H. L. Zhang, Astrophys. J, 335, 516 (1988)
[35] T. Hara, K. Ando, N. Kusakabe, H. Yashiro and Y. Aoyagi, Jpn. J. Appl. Phys, **28**, 1010 (1989)
[36] A. Carillon, M. J. Edward, M. Grande, M. J. de C. Henshow, P. Jaegle, G. Jamelot, M. H. Key, G. P. Keihn, A. Klsnick, C. K. S. Lewis, D. O'Niell, G. J. Pert, S. A. Ramsden, C. E. Regan, S. J. Rose, R. Smith, and O. Willi, J. Phys. B**23**, 147 (1990)

Table II-1. Fitting parameters for the energy of the excited level measured from the ground state (eV)

transition	C_1	C_2	C_3	C_4
$2s^2S$-$2p^2P_{1/2}$	2.02360	7.63516 (-3)	4.03435 (-4)	3.50523 (-6)
$2s^2S$-$2p^2P_{3/2}$	1.86034	2.09641 (-2)	9.96515 (-4)	6.54990 (-5)
$2s^2S$-$3s^2S_{1/2}$	2.03012	1.86053	2.15764 (-3)	
$2s^2S$-$3p^2P_{1/2}$	2.57010	1.86074	2.18833 (-3)	
$2s^2S$-$3p^2P_{3/2}$	2.64457	1.84622	3.02400 (-3)	
$2s^2S$-$3d^2D_{3/2}$	2.80616	1.85040	2.95088 (-3)	
$2s^2S$-$3d^2D_{5/2}$	2.82538	1.84642	3.19623 (-3)	
$2s^2S$-$4s^2S$	2.50127	2.51293	2.80191 (-3)	
$2s^2S$-$4p^2P$	2.72231	2.51292	2.82370 (-3)	
$2s^2S$-$4d^2D$	2.82148	2.50884	3.13175 (-3)	
$2s^2S$-$4f^2F$	2.85063	2.50632	3.24800 (-3)	
$2s^2S$-$5s^2S$	2.66090	2.81601	3.04306 (-3)	
$2s^2S$-$5p^2P$	2.76940	2.81645	3.04064 (-3)	
$2s^2S$-$5d^2D$	2.81834	2.81454	3.19541 (-3)	
$2s^2S$-$5f^2F$	2.83717	2.81267	3.27143 (-3)	
$2s^2S$-$5g^2G$	2.85217	2.81149	3.30877 (-3)	

* (-p) means $\times 10^{-p}$.

Table II-2. Fitting parameters for the absorption oscillator strength.

transition	C_1	C_2	C_3	C_4
2^2S-$3^2P_{1/2}$	0.13796	-0.15043	-0.38835	1.0560
2^2S-$3^2P_{3/2}$	0.24421	6.8560	-19.572	2.1160
2^2S-4^2P	9.4591 (-2)	0.75369	-2.3790	1.9990
2^2S-5^2P	7.5024 (-2)	-0.22318	-3.6884 (-2)	8.8471 (-3)
$2^2P_{1/2}$-3^2S	0.18187	0.29300	-0.15963	-1.0173 (-2)
$2^2P_{1/2}$-4^2S	0.14546	5.5335 (-2)	-0.14093	-1.9114 (-3)
$2^2P_{1/2}$-5^2S	0.13893	1.9218 (-2)	-0.13713	-7.6803 (-4)
$2^2P_{1/2}$-$3^2D_{3/2}$	0.10485	-2.0162	0.56994	6.6767 (-3)
$2^2P_{1/2}$-$4^2D_{3/2}$	0.19421	2.7930 (-2)	-6.8550 (-2)	-1.3520 (-2)
$2^2P_{1/2}$-$5^2D_{3/2}$	0.16453	4.6981 (-2)	-0.11788	-3.4209 (-3)
$2^2P_{3/2}$-3^2S	0.16013	0.34780	-0.14292	1.39333 (-3)
$2^2P_{3/2}$-4^2S	0.14563	6.3087 (-2)	-0.14200	4.2164 (-4)
$2^2P_{3/2}$-5^2S	0.14337	2.1549 (-2)	-0.14185	1.8398 (-5)
$2^2P_{3/2}$-$3^2D_{3/2}$	6.7235 (-2)	0.14974	-0.40673	1.8056
$2^2P_{3/2}$-$3^2D_{5/2}$	-0.18942	-1.4983	0.76625	-1.0197 (-2)
$2^2P_{3/2}$-4^2D	0.19102	2.4880 (-2)	-6.5457 (-2)	-1.2836 (-2)
$2^2P_{3/2}$-5^2D	0.16450	4.1760 (-2)	-0.11738	-4.7800 (-3)
3^2S-4^2P	-1.2232	-2.0861	1.4285	-4.3588 (-2)
3^2S-5^2P	0.1481	-5.4063 (-2)	-0.2166	0.58345
$3^2P_{1/2}$-4^2S	4.6238 (-2)	-0.27642	3.2633	2.3769
$3^2P_{1/2}$-5^2S	1.2355 (-2)	-0.80070	6.3012	2.7435
$3^2P_{1/2}$-4^2D	-2.1699	-0.52680	2.7021	-6.9282 (-3)
$3^2P_{3/2}$-5^2D	0.23246	-1.9082 (-2)	-0.10674	3.9274 (-2)
$3^2P_{3/2}$-4, 5 ^2S	same as $3^2P_{1/2}$			
$3^2P_{3/2}$-4, 5 ^2D	same as $3^2P_{1/2}$			
$3^2D_{3/2}$-4^2P	7.2805 (-3)	1.7312	-16.312	2.9344
$3^2D_{3/2}$-5^2P	1.8186 (-3)	0.25527	-2.3983	2.9326
$3^2D_{3/2}$-4^2F	1.015	0.0000	0.0000	0.0000
$3^2D_{3/2}$-5^2F	0.1565	0.0000	0.0000	0.0000

Table II-2. (Continued)

transition	C_1	C_2	C_3	C_4
$3^2D_{5/2}$-4, 5 ^2P	same as $3^2D_{3/2}$			
$3^2D_{5/2}$-4, 5 ^2F	same as $3^2D_{3/2}$			
4^2S-5^2P	-3.0129	-1.5386	3.1378	-3.2640 (-2)
4^2P-5^2S	4.8882 (-2)	6.2580	-66.580	3.0805
4^2P-5^2D	-2.4693	-0.13835	2.9084	-1.5923 (-2)
4^2D-5^2P	2.4435 (-2)	2.2772	-23.664	3.0081
4^2D-5^2F	0.8855	0.0000	0.0000	0.0000
4^2F-5^2D	8.8392 (-3)	2.5175 (-2)	-0.64736	3.5608
4^2F-5^2G	1.346	0.0000	0.0000	0.0000

Table II-3. Absorption Oscillator Strength

transition	$2^2S_{1/2}$ - n^2P	$2^2P_{1/2,3/2}$ - n^2S	$2^2P_{1/2,3/2}$ - n^2D	$3^2S_{1/2}$ - n^2P
a	-3.8	-3.48	-3.50	-4.25
transition	$3^2P_{1/2,3/2}$ - n^2S	$3^2p_{1/2,3/2}$ - n^2D	$3^2D_{3/2,5/2}$ - n^2P	$3^2D_{3/2,5/2}$ - n^2F
a	-4.08	-4.21	-5.40	-4.41
transition	4^2S - n^2P	4^2P- n^2S	4^2P - n^2D	4^2D - n^2P
a	-5.08	-5.95	-5.27	-6.83
transition	4^2D - n^2F	4^2F- n^2D	4^2F - n^2G	
a	-6.00	-5.94	-5.95	

Table II-4. Absorption Oscillator Strength for Δn=0 transitions

transition	$3^2S_{1/2}$ - $3^2P_{1/2}$	$3^2S_{1/2}$ - $3^2P_{3/2}$	$3^2P_{1/2}$ - $3^2D_{3/2}$	$3^2P_{3/2}$ - $3^2D_{3/2}$
O.S.	0.112	0.224	0.0488	4.78 (-3)
transition	$3^2P_{3/2}$ - $3^2D_{5/2}$	4^2S - 4^2P	4^2P - 4^2D	4^2D - 4^2F
O.S.	0.0433	0.4616	8.555 (-2)	2.374 (-3)
transition	5^2S - 5^2P	5^2P - 5^2D	5^2D - 5^2F	5^2F - 5^2G
O.S.	0.5860	0.1184	5.606 (-3)	4.18 (-4)

O.S. means the oscillator strength.

Table II-5. Excitation cross section fitting parameters.

transition	A	B	C	D	Ref
2^2S - 2^2P	2.234 (-1)	5.625 (1)	- 1.648	3.00 (-2)	3
2^2S - 3^2S	0.000	1.481	5.694 (-1)	6.50 (-2)	3
2^2S - 3^2P	1.706 (-1)	- 5.800 (-1)	6.250 (-2) 1.800 (1)	1.40 (-2) 9.60 (-2)	3
2^2S - 3^2D	0.000	3.470	- 5.860 (-2)	1.50 (-2)	3
2^2S - 4^2S	0.000	2.961 (-1)	- 2.278 (-2)	3.70 (-2)	3
2^2S - 4^2P	9.634 (-3)	1.760 (-1)	- 6.534 (-3)	8.00 (-2)	3
2^2S - 4^2D	0.000	6.030 (-1)	- 5.400 (-3)	1.30 (-2)	3
2^2S - 4^2F	0.000	1.424 (-1)	0.000	0.00	3
2^2S - 5^2S	0.000	1.139 (-1)	- 2.278 (-3)	1.98 (-2)	3
2^2S - 5^2P	4.043 (-3)	8.610 (-2)	- 2.468 (-3)	6.50 (-3)	3
2^2S - 5^2D	0.000	2.097 (-1)	- 1.502 (-3)	1.20 (-2)	3
2^2S - 5^2F	0.000	8.030 (-2)	- 1.141 (-4)	1.00 (-2)	3
2^2S - 5^2G	0.000	3.417 (-3)	5.695 (-3)	4.00 (-2)	3
2^2P - 3^2S	5.826 (-3)	1.642 (-1)	- 4.358 (-3)	7.90 (-3)	3
2^2P - 3^2P	0.000	1.987	0.000	0.000	3
2^2P - 3^2D	1.240 (-1)	7.270	1.280 (-1)	9.20 (-3)	3
2^2P - 4^2S	8.076 (-4)	3.911 (-2)	- 4.632 (-4)	5.00 (-3)	3
2^2P - 4^2P	0.000	3.673 (-1)	1.708 (-2)	2.98 (-2)	3
2^2P - 4^2D	1.756 (-2)	1.279	- 1.200 (-2)	7.20 (-3)	3
2^2P - 4^2F	0.000	2.707 (-1)	- 2.500 (-3)	9.00 (-3)	3
2^2P - 5^2S	2.764 (-4)	1.726 (-2)	- 1.534 (-4)	3.88 (-3)	3
2^2P - 5^2P	0.000	1.481 (-1)	1.162 (-2)	3.00 (-2)	3
2^2P - 5^2D	5.876 (-3)	5.340 (-1)	- 5.200 (-3)	7.20 (-3)	3
2^2P - 5^2F	0.000	1.139 (-1)	0.000	0.000	3
2^2S - 5^2G	0.000	5.125 (-3)	6.834 (-2)	6.99 (-2)	3
3^2S - 4^2S	0.000	4.320	0.000	0.000	13
3^2S - 4^2P	1.627 (-1)	1.263 (1)	- 2.721 (-1) - 1.174	1.28 (-2) 6.01 (-2)	13
3^2S - 4^2D	0.000	8.200	- 3.209 (-1)	3.00 (-2)	13
3^2S - 4^2F	0.000	3.880	0.000	0.00	13
3^2S - 5^2S	0.000	7.652 (-1)	0.000	0.00	13
3^2S - 5^2P	1.638 (-1)	2.270 (-1)	- 2.800 (-2)	2.00 (-2)	13
3^2S - 5^2D	0.000	1.260	- 1.000 (-2)	2.00 (-2)	13
3^2S - 5^2F	0.000	3.270 (-1)	6.843 (-2)	4.73 (-2)	13
3^2S - 5^2G	0.000	7.830 (-1)	1.580 (-1)	6.70 (-2)	13

Table II-5. (Continued)

transition	A	B	C	D	ref
$3^2P - 4^2S$	3.758 (-2)	7.956 (-1)	- 1.621 (-2) - 5.930 (-2)	1.12 (-1) 5.20 (-2)	13
$3^2P - 4^2P$	0.000	5.030	- 3.998 (-2)	2.50 (-2)	13
$3^2P - 4^2D$	0.3014	6.100	- 2.170 (-1)	2.41 (-2)	13
$3^2P - 4^2F$	0.000	1.013 (1)	- 4.000 (-1)	4.00 (-2)	13
$3^2P - 5^2S$	9.502 (-3)	- 3.300 (-1)	3.500 (-2)	5.20 (-2)	13
$3^2P - 5^2P$	0.000	9.697(-1)	7.600 (-1)	1.80 (-1)	13
$3^2P - 5^2D$	9.832 (-2)	- 2.856	1.476 (-1)	4.40 (-2)	13
$3^2P - 5^2F$	0.000	7.921 (-1)	1.134	1.20 (-1)	13
$3^2P - 5^2G$	0.000	1.090	1.130	1.20 (-1)	13
$3^2D - 4^2S$	0.000	9.000 (-1)	7.000 (-3)	2.00 (-1)	13
$3^2D - 4^2P$	8.954 (-3)	4.900 (-1)	- 6.600 (-3)	1.55 (-2)	13
$3^2D - 4^2D$	0.000	4.170	4.950 (-2)	1.00 (-1)	13
$3^2D - 4^2F$	5.776 (-1)	2.049 (1)	- 4.200 (-1)	1.50 (-2)	13
$3^2D - 5^2S$	0.000	2.280 (-2)	8.400 (-3)	5.00 (-2)	13
$3^2D - 5^2P$	2.144 (-3)	1.800 (-2)	3.300 (-2)	4.30 (-2)	13
$3^2D - 5^2D$	0.000	7.600 (-1)	1.240 (-1)	5.50 (-2)	13
$3^2D - 5^2F$	2.448 (-1)	- 5.884	1.402 (-1) 4.401	1.50 (-2) 1.02 (-1)	13
$3^2D - 5^2G$	0.000	1.588	- 1.881 (-2)	1.50 (-2)	13
$4^2S - 5^2S$	0.000	2.340 (1)	0.000	0.000	13
$4^2S - 5^2P$	1.299	- 9.879	- 7.421	1.56 (-1)	13
$4^2S - 5^2D$	0.000	2.233 (1)	- 7.493 (-1)	2.50 (-2)	13
$4^2S - 5^2F$	0.000	1.046 (1)	0.000	0.000	13
$4^2S - 5^2G$	0.000	9.112	0.000	0.000	13
$4^2P - 5^2S$	7.736 (-2)	0.000	4.408 (-1)	1.55 (-1)	13
$4^2P - 5^2P$	0.000	2.847 (1)	0.000	0.000	13
$4^2P - 5^2D$	2.320	- 3.234	8.876	1.40 (-1)	13
$4^2P - 5^2F$	0.000	3.840 (1)	- 3.102	6.00 (-2)	13
$4^2P - 5^2G$	0.000	1.481 (1)	0.000	0.00	13
$4^2D - 5^2S$	0.000	4.320 (-1)	- 1.000 (-2)	5.50 (-2)	12

Table II-5. (Continued)

transition	*A*	*B*	*C*	*D*	Ref
$4^2D - 5^2P$	1.642 (-1)	- 2.897	2.570 (-1) 1.164	4.50 (-2) 1.45 (-1)	13
$4^2D - 5^2D$	0.000	1.396 (1)	- 1.200 (-1)	5.50 (-2)	12
$4^2D - 5^2F$	3.854	- 6.663 (1)	5.911 2.401 (1)	4.50 (-2) 1.45 (-1)	12
$4^2D - 5^2G$	0.000	2.247 (1)	- 9.480 (-1)	5.50 (-2)	12
$4^2F - 5^2S$	0.000	6.282 (-2)	5.180 (-2)	1.25 (-1)	12
$4^2F - 5^2P$	0.000	3.021 (-1)	1.498 (-1)	1.25 (-1)	12
$4^2F - 5^2D$	3.959 (-2)	5.031 (-1)	1.000	1.45 (-1)	12
$4^2F - 5^2F$	0.000	1.119 (1)	8.680 (-1)	1.25 (-1)	12
$4^2F - 5^2G$	5.858	-7.367	7.064 3.834 (1)	4.50 (-2) 1.45 (-1)	12

Table II-6. The fitting parameters for the *l*-changing process

transition	*A*	*B*	*C*	*D*	Ref
3^2S-3^2P	5.345	2.180 (2)	4.172 (1)	1.56 (-1)	13
4^2S-4^2P	2.511 (1)	7.912 (2)	4.960 (2)	2.86 (-1)	13
5^2S-5^2P	6.308 (1)	1.962 (3)	1.240 (3)	2.86 (-1)	13

Table II-7. Deexcitation Rate Coefficients

transition	K	L	M	N	P	factor
2^2S - 2^2P	25.0	0.55	60.2	0.0	0.0	1.0e-15
2^2S - 3^2S	290.0	0.62	600.	0.0	0.0	1.0e-17
2^2S - 3^2P	11.0	0.2	185.	0.0	0.0	1.0e-17
2^2S - 3^2D	58.0	0.5	360.	0.0	0.0	1.0e-17
2^2S - 4^2S	48.0	0.6	200.	0.0	0.0	1.0e-17
2^2S - 4^2P	11.7	0.43	50.0	5.7	0.01	1.0e-17
2^2S - 4^2D	14.0	0.55	77.1	0.0	0.0	1.0e-17
2^2S - 4^2F	35.0	0.6	150.0	0.0	0.0	1.0e-18
2^2S - 5^2S	14.5	0.58	120.0	0.0	0.0	1.0e-17
2^2S - 5^2P	10.0	0.5	15.0	-4.15	0.005	1.0e-17
2^2S - 5^2D	8.3	0.62	21.3	0.0	0.0	1.0e-17
2^2S - 5^2F	38.0	0.7	40.0	0.0	0.0	1.0e-18
2^2S - 5^2G	28.0	0.8	70.0	560.0	0.52	1.0e-19
2^2P - 3^2S	101.0	0.5	403	-44.0	0.01	1.0e-17
2^2P - 3^2P	165.0	0.5	2640	0.0	0.0	1.0e-17
2^2P - 3^2D	63.0	0.5	231.6	-12.0	0.01	1.0e-16
2^2P - 4^2S	15.5	0.5	80.0	-3.0	0.005	1.0e-16
2^2P - 4^2P	33.25	0.5	550.0	8.0	0.01	1.0e-17
2^2P - 4^2D	12.0	0.5	78.0	-3.0	0.005	1.0e-16
2^2P - 4^2F	9.5	0.5	50.0	0.0	0.0	1.0e-17
2^2P - 5^2S	800.0	0.5	2.0e3	-160.0	0.003	1.0e-19
2^2P - 5^2P	34.8	0.65	130.5	0.0	0.0	1.0e-17
2^2P - 5^2D	32.0	0.45	238.0	0.0	0.0	1.0e-17
2^2P - 5^2F	12.0	0.65	45.0	0.0	0.0	1.0e-17
2^2P - 5^2G	60.0	0.7	240.5	0.0	0.0	1.0e-19
3^2S - 4^2S	6.00	0.5	74.0	1.0	0.01	1.0e-15
3^2S - 4^2P	70.5	0.5	30.0	-30.0	0.007	1.0e-16
3^2S - 4^2D	22.5	0.5	110.0	0.0	0.00	1.0e-16
3^2S - 4^2F	8.00	0.5	100.0	2.0	0.01	1.0e-16

Table II-7. (Continued)

transition	*K*	*L*	*M*	*N*	*P*	factor
3^2S - 5^2S	13.0	0.6	45.0	0.0	0.0	1.0e-16
3^2S - 5^2P	10.0	0.5	0.5	-4.2	0.05	1.0e-16
3^2S - 5^2D	48.0	0.6	80.0	0.0	0.0	1.0e-17
3^2S - 5^2F	18.0	0.7	0.0	270.0	0.4	1.0e-17
3^2S - 5^2G	18.0	0.62	50.0	0.0	0.0	1.0e-17
3^2P - 4^2S	17.2	0.35	77.0	-7.3	0.01	1.0e-16
3^2P - 4^2P	280.0	0.7	350.0	0.0	0.0	1.0e-16
3^2P - 4^2D	55.0	0.3	500.0	0.0	0.0	1.0e-16
3^2P - 4^2F	110.0	0.6	180.3	0.0	0.0	1.0e-16
3^2P - 5^2S	56.7	0.5	83.3	-19.3	0.0038	1.0e-17
3^2P - 5^2P	220.0	0.65	450.0	0.0	0.0	1.0e-17
3^2P - 5^2D	24.8	0.5	36.12	-6.4	0.0045	1.0e-16
3^2P - 5^2F	8.0	0.65	20.0	0.0	0.0	1.0e-16
3^2P - 5^2G	8.0	0.65	20.0	0.0	0.0	1.0e-16
3^2D - 4^2S	140.0	0.6	600.0	0.0	0.0	1.0e-17
3^2D - 4^2P	145.0	0.5	1100.0	-25.0	0.01	1.0e-17
3^2D - 4^2D	40.0	0.85	400.0	-2.0	0.01	1.0e-17
3^2D - 4^2F	50.0	0.5	190.0	-13.0	0.01	1.0e-15
3^2D - 5^2S	24.0	0.62	144.0	0.0	0.0	1.0e-17
3^2D - 5^2P	24.0	0.55	230.0	4.0 (3)	0.8	1.0e-17
3^2D - 5^2D	170.0	0.65	800.0	0.0	0.0	1.0e-17
3^2D - 5^2F	400.0	0.5	1900.0	-70.0	0.005	1.0e-17
3^2D - 5^2G	8.0	0.5	90.0	850.0	0.32	1.0e-16
4^2S - 5^2S	50.0	0.65	700.0	4.0e4	0.8	1.0e-15
4^2S - 5^2P	6.0	0.42	0.0	112.0	0.22	1.0e-15
4^2S - 5^2D	7.0	0.6	66.0	84.0	0.2	1.0e-15
4^2S - 5^2F	6.0	0.7	60.0	78.0	0.2	1.0e-15
4^2S - 5^2G	1.5	0.6	50.0	59.0	0.2	1.0e-15
4^2P - 5^2S	60.0	0.55	-1	-24.3	0.013	1.0e-15
4^2P - 5^2P	65.0	0.65	216.0	0.0	0.0	1.0e-15

Table II-7. (Continued)

transition	K	L	M	N	P	factor
4^2P - 5^2D	45.0	0.5	50.0	-12.0	0.01	1.0e-15
4^2P - 5^2F	36.0	0.65	50.0	0.0	0.0	1.0e-15
4^2P - 5^2G	12.0	0.65	45.0	0.0	0.0	1.0e-15
4^2D - 5^2S	50.0	0.62	190.0	0.0	0.0	1.0e-16
4^2D - 5^2P	50.0	0.5	60.0	100.0	0.20	1.0e-16
4^2D - 5^2D	298.0	0.65	1490	0.0	0.0	1.0e-16
4^2D - 5^2F	300.0	0.4	0.0	1000	0.2	1.0e-16
4^2D - 5^2G	240.0	0.6	995.0	0.0	0.0	1.0e-16
4^2F - 5^2S	50.0	0.88	302.0	784.0	0.5	1.0e-16
4^2F - 5^2P	24.0	0.7	333.0	0.0	0.0	1.0e-16
4^2F - 5^2D	20.0	0.5	487.0	0.0	0.0	1.0e-16
4^2F - 5^2F	250.0	0.65	1800	0.0	0.0	1.0e-16
4^2F - 5^2G	120.0	0.5	380	-25.0	0.005	1.0e-15

Table II-8. Deexcitation Rate Coefficients for l-changing transition

transition	K	L	M	N	P	factor
3^2S-3^2P	2.5	0.6	0.0	4.1	0.3	1.0e-13
3^2P-3^2D	3.5	0.7	0.0	37.0	0.5	1.0e-13
4^2S-4^2P	5.0	0.5	20.0	0.0	0.0	1.0e-13
4^2P-4^2D	1.3	0.6	0.0	3.0	0.4	1.0e-12
4^2D-4^2F	1.0	0.6	0.0	2.0	0.3	1.0e-12
5^2S-5^2P	2.7	0.6	0.0	5.0	0.3	1.0e-12
5^2P-5^2D	3.3	0.6	0.0	6.3	0.3	1.0e-12
5^2D-5^2F	4.1	0.6	0.0	8.0	0.3	1.0e-12
5^2F-5^2G	4.3	0.6	0.0	8.23	0.3	1.0e-12

Table II-9. Dielectronic recombination rate coefficient for OVII → OVI.

Dielectronic recombination rate coefficient by ref [29]

$$\alpha_d(1,nl) = \sum_p^{\infty} Z(p,nl)\frac{A_a A_{r1}}{A_a + A_{r2}}$$

$$= \sum_p^{\infty} \frac{g_z(p,nl)}{2g_z}\left(\frac{h^2}{2\pi mkT_e}\right)^{1.5} \exp[-E(p,nl)/T_e]\frac{A_a A_{r1}}{A_a + A_{r2}}$$

$$= 2.07\times10^{-16}\sum_p^{\infty}\frac{g_z(p,nl)}{g_z}T_e^{-1.5}\exp[-E(p,nl)/T_e]\frac{A_a A_{r1}}{A_a + A_{r2}}$$

$$E(p,nl)\ [\mathrm{eV}] = [E(p)-E(nl)]\times[(z-2)/(8-2)]^2$$

where $E(p)$ and $E(nl)$ are the energy of the level p of heliumlike oxygen ion with respect to its ground state and the ionization potential of the level nl of lithiumlike oxygen ion, respectively. T_e is in kelvin.

The transition to the 2^2P

transition	$g_Z(p, nl)$	autoionization A_a	radiative decay A_{r1}	rad. decay A_{r2}
a	4	9.44e10	3.97e12	4.71e12
b	4	9.44e10	7.21e11	4.71e12
j	6	9.80e13	1.48e12	1.48e12
k	4	9.79e13	1.29e12	1.49e12
l	4	9.79e13	1.88e11	1.49e12
m	2	8.71e12	9.28e11	1.38e12
n	2	8.71e12	4.37e11	1.38e12
p	2	1.02e14	1.22e11	1.90e11

The transitions are expressed by Gabriel notation

The transition to the 3^2S

transition	$g_Z(p, nl)$	A_a	A_{r1}	A_{r2}
$1s^2 3s$ - $1s2p3s$	6	6.9e12	2.47e12	2.73e12
- $1s2p3s$	6	2.65e13	3.68e11	3.97e11
- $1s2s3p$	6	4.45e11	2.13e11	6.43e11
- $1s2p3d$	6	9.06e10	1.38e11	3.43e11

The transition to the 3^2P

transition	$g_Z(p, nl)$	A_a	A_{r1}	A_{r2}
$1s^2 3p$ - $1s2p3p$	2	5.87e12	2.27e12	2.31e12
	2	1.61e12	6.10e11	1.55e12
	10	2.43e13	2.39e12	2.57e12
	10	1.75e13	7.66e11	1.35e12
- $1s2s3s$	2	1.68e13	3.43e11	4.27e11

The transition to the 3^2D

transition	$g_Z(p, nl)$	A_a	A_{r1}	A_{r2}
$1s^2 3d$ - $1s2p3d$	6	7.65e10	2.93e12	2.93e12
	6	9.06e10	1.11e11	3.43e11
	14	6.32e12	2.63e12	2.76e12
	14	7.65e10	6.09e11	6.73e12
- $1s2p3s$	6	2.65e13	1.22e11	6.43e11

The transition to the 4^2S

Transition	$g_Z(p, nl)$	A_a	A_{r1}	A_{r2}
$1s^2 4s$ - $1s2p4s$	6	1.89e12	2.60e12	2.71e12

The transition to the 4^2P

transition	$g_Z(p, nl)$	A_a	A_{r1}	A_{r2}
$1s^2 4p$ - $1s2p4p$	2	1.16e12	2.92e12	3.00e12
-	10	7.07e12	3.12e12	3.29e12
- $1s2s4s$	10	6.01e12	1.49e11	1.90e11

The transition to the 4^2D

transition	$g_Z(p, nl)$	A_a	A_{r1}	A_{r2}
$1s^2 4d$ - $1s2p4d$	6	1.62e11	3.19e12	3.28e12
	6	2.19e11	3.07e10	3.07e10
	14	3.20e12	3.13e12	3.13e12
	14	3.01e11	5.39e10	9.47e10

The transition to the 4^2F

transition	$g_Z(p, nl)$	A_a	A_{r1}	A_{r2}
$1s^2 4f$ - $1s2p4f$	10	4.47e10	3.33e12	3.36e12
-	18	1.46e11	3.28e12	3.30e12

The transition to the levels with n=5

transition	$g_Z(p, nl)$	A_a	A_{r1}	A_{r2}
$1s^2 5s$-$1s2p5s$	6	2.80e11	3.26e12	3.32e12
$1s^2 5p$-$1s2p5p$	2	1.05e12	3.27e12	3.32e12
	10	3.39e12	3.23e12	3.37e12
$1s^2 5d$-$1s2p5d$	6	1.28e11	3.31e12	3.37e12
	14	1.70e12	3.27e12	3.30e12
$1s^2 5f$-$1s2p5f$	10	5.95e10	3.36e12	3.38e12
	18	1.17e11	3.30e12	3.31e12
$1s^2 5g$-$1s2p5g$	22	9.53e9	3.30e12	3.31e12

For the transition to the level with $n \geq 6$, we assume hydrogenic approximation, and the autoionization probability is given as

$$A_a = \frac{4}{h\, n^3} \frac{R}{g(p,nl)} z^2 \Omega \ (1s^2 \rightarrow 1s\, 2p)$$

where $z^2 \Omega \ (1s^2 \rightarrow 1s\, 2p) = 2.355$ at the threshold.

transition	$g_Z(p, nl)$	A_a	A_{r1}	A_{r2}
$1s^2 n$-$1s2pn$	$2n^2+4n$		3.30e12	3.30e12

TABLE III-1 Energy Level of Li-like Al

state	Lindgard	Zhang	Duston	Kelly	Evaluated	Fitting
2s	0.0	0.0	0.0	0.0	0.00	0.0
2p	22.54	22.300	22.30	22.301	22.30	22.36
3s	250.50	250.55	250.51	250.50	250.50	250.33
3p	256.70	256.71	256.64	256.63	256.63	256.45
3d	258.94	259.04	258.93	258.91	258.91	258.73
4s	335.44	335.59	335.47	335.44	335.44	335.31
4p	338.06	338.12	338.07	338.06	338.06	337.77
4d	338.98	339.12	339.02	338.97	338.97	338.77
4f	339.03	339.27	339.10	339.10	339.10	338.94
5s	374.38	374.37	374.10	374.38	374.38	374.06
5p	375.62	375.65	375.64	375.62	375.62	375.30
5d	376.11	376.16	376.14	376.10	376.10	375.81
5f	376.14	376.24	376.16		376.16	375.90
5g	376.21	376.30	376.17		376.18	375.97
6s	395.24		395.26		395.24	396.17
6p	395.94		395.96	395.94	395.94	
6d	396.29		396.31	396.28	396.28	
6f	396.29		396.32		396.32	
6g	396.33		396.36		396.33	
6h			396.38		396.33	
7s	407.78				407.78	408.29
7p	408.15			408.15	408.15	
7d	408.43			408.43	408.43	
7f	408.44				408.46	
7g	408.47				408.46	
7h					408.46	
7i						
8s	415.88				415.88	416.16
8p	416.14			416.14	416.14	
8d	416.34			416.33	416.34	
8f	416.32				416.36	
8g	416.34				416.36	
9s	421.42				421.29	421.56
9p	421.47			421.47	421.47	
9d	421.72				421.61	
9f	421.73				421.62	
9g	421.74				421.62	
10s	425.36				425.39	425.42
10p	425.52				425.52	
10d	425.59				425.62	
10f	425.59				425.62	
10g	425.60					
free	442.06			442.08	442.08	441.86

TABLE III-2 Oscillator Strength of Li-lika Al

Lindgard		Guennou	Zhang	Recom	H-like	Recm/H	Fitting
2s-2p	1.153E-1		0.1168	1.17E-1			1.19E-1
2s-3p	3.281E-1	3.322E-1	0.3337	3.35E-1	4.349E-1	0.77	3.28E-1
2s-4p	8.624E-2	8.659E-2	0.0878	8.73E-2	1.028E-1	0.85	8.66E-2
2s-5p	3.638E-2	3.640E-2	0.0369	3.69E-2	4.193E-2	0.88	3.73E-2
2s-6p	1.922E-2	1.904E-2		1.92E-2	2.163E-2	0.89	
2s-7p	1.159E-2	1.130E-2		1.13E-2	1.274E-2	0.89	
2s-8p	7.456E-3			7.28E-3	8.181E-3	0.89	
2s-9p	5.349E-3			4.97E-3	5.583E-3	0.89	
2s-10p	3.601E-3			3.55E-3	3.988E-3	0.89	
2p-3s	2.152E-2	2.127E-2	0.0208	2.08E-2	1.359E-2	1.53	2.18E-2
2p-4s	4.568E-3	4.417E-3	0.0044	4.42E-3	3.045E-3	1.45	4.54E-3
2p-5s	1.748E-3	1.721E-3	0.0017	1.70E-3	1.213E-3	1.4	1.82E-3
2p-6s	8.970E-4	8.670E-4		8.53E-4	6.180E-4	1.38	
2p-7s	5.218E-4	5.034E-4		4.95E-4	3.613E-4	1.37	
2p-8s	3.325E-4			3.16E-4	2.308E-4	1.37	
2p-9s	2.252E-4			2.15E-4	1.570E-4	1.37	
2p-10s	1.603E-4			1.53E-4	1.119E-4	1.37	
2p-3d	6.689E-1	6.727E-1	0.6474	6.47E-1	6.958E-1	0.93	6.66E-1
2p-4d	1.225E-1	1.230E-1	0.1235	1.23E-1	1.218E-1	1.01	1.24E-1
2p-5d	4.523E-2	4.550E-2	0.046	4.57E-2	4.437E-2	1.03	4.54E-2
2p-6d	2.228E-2	2.235E-2		2.25E-2	2.163E-2	1.04	
2p-7d	1.272E-2	1.279E-2		1.28E-2	1.233E-2	1.04	
2p-8d	8.090E-3			8.07E-3	7.756E-3	1.04	
2p-9d	5.409E-3			5.43E-3	5.221E-3	1.04	
2p-10d	3.834E-3			3.84E-3	3.693E-3	1.04	
3s-3p	1.954E-1			1.95E-1			1.93E-1
3s-4p	3.593E-1	3.599E-1		3.59E-1	4.847E-1	0.74	3.56E-1
3s-5p	9.931E-2	9.843E-2		9.80E-2	1.210E-1	0.81	1.00E-1
3s-6p	4.423E-2	4.355E-2		4.37E-2	5.139E-2	0.85	
3s-7p	2.447E-2	2.363E-2		2.35E-2	2.737E-2	0.86	
3s-8p	1.487E-2			1.44E-2	1.655E-2	0.87	
3s-9p	1.051E-2			9.45E-3	1.086E-2	0.87	
3s-10p	6.725E-3			6.57E-3	7.554E-3	0.87	
3p-4s	5.050E-2	4.869E-2		4.87E-2	3.225E-2	1.51	4.95E-2
3p-5s	1.061E-2	1.045E-2		1.05E-2	7.428E-3	1.41	1.00E-2
3p-6s	4.315E-3	4.161E-3		4.15E-3	3.032E-3	1.37	
3p-7s	2.228E-3	2.140E-3		2.15E-3	1.579E-3	1.36	
3p-8s	1.323E-3			1.28E-3	9.412E-4	1.36	
3p-9s	8.560E-4			8.32E-4	6.120E-4	1.36	
3p-10s	5.903E-4			5.75E-4	4.227E-4	1.36	
3p-3d	3.060E-2			3.10E-2			3.13E-2
3p-4d	5.810E-1	5.794E-1		5.81E-1	6.183E-1	0.94	5.86E-1
3p-5d	1.361E-1	1.361E-1		1.36E-1	1.392E-1	0.98	1.38E-1
3p-6d	5.568E-2	5.564E-2		5.56E-2	5.614E-2	0.99	

TABLE III-2 Continued

Lindgard		Guennou	Zhang	Recom	H-like	Recm/H	Fitting
3p-7d	2.899E-2	2.895E-2		2.90E-2	2.901E-2	1	
3p-8d	1.730E-2			1.72E-2	1.721E-2	1	
3p-9d	1.121E-2			1.12E-2	1.115E-2	1	
3p-10d	7.746E-3			7.69E-3	7.686E-3	1	
3d-4p	1.393E-2	1.358E-2		1.36E-2	1.099E-2	1.24	1.33E-2
3d-5p	2.767E-3	2.411E-3		2.70E-3	2.210E-3	1.22	2.89E-3
3d-6p	1.086E-3	1.017E-3		1.02E-3	8.420E-4	1.21	
3d-7p	5.784E-4	5.129E-4		5.10E-4	4.212E-4	1.21	
3d-8p	3.329E-4			2.96E-4	2.448E-4	1.21	
3d-9p	2.681E-4			1.89E-4	1.564E-4	1.21	
3d-10p	1.373E-4			1.29E-4	1.067E-4	1.21	
3d-4f	1.018E+0	1.017E+0		1.02E+0	1.018E+0	1	1.02E+0
3d-5f	1.563E-1	1.566E-1		1.57E-1	1.566E-1	1	1.57E-1
3d-6f	5.382E-2	5.410E-2		5.39E-2	5.389E-2	1	
3d-7f	2.551E-2	2.570E-2		2.56E-2	2.559E-2	1	
3d-8f	1.439E-2			1.44E-2	1.442E-2	1	
3d-9f	8.993E-3			9.03E-3	9.034E-3	1	
3d-10f	6.058E-3			6.08E-3	6.081E-3	1	
4s-4p	2.767E-1			2.77E-1			2.52E-1
4s-5p	3.907E-1	3.967E-1		3.97E-1	5.442E-1	0.73	3.84E-1
4s-6p	1.115E-1	1.107E-1		1.10E-1	1.381E-1	0.8	
4s-7p	5.101E-2	4.972E-2		4.95E-2	5.965E-2	0.83	
4s-8p	2.778E-2			2.68E-2	3.227E-2	0.83	
4s-9p	1.869E-2			1.64E-2	1.980E-2	0.83	
4s-10p	1.119E-2			1.09E-2	1.317E-2	0.83	
4p-5s	7.877E-2	7.828E-2		7.83E-2	5.291E-2	1.48	8.30E-2
4p-6s	1.731E-2	1.696E-2		1.70E-2	1.234E-2	1.38	
4p-7s	6.942E-3	6.840E-3		6.83E-3	5.094E-3	1.34	
4p-8s	3.595E-3			3.59E-3	2.682E-3	1.34	
4p-9s	2.136E-3			2.17E-3	1.617E-3	1.34	
4p-10s	1.392E-3			1.42E-3	1.062E-3	1.34	
4p-4d	5.376E-2			5.40E-2			6.67E-2
4p-5d	5.606E-1	5.619E-1		5.61E-1	6.093E-1	0.92	5.53E-1
4p-6d	1.417E-1	1.426E-1		1.41E-1	1.485E-1	0.95	
4p-7d	6.051E-2	6.093E-2		6.07E-2	6.255E-2	0.97	
4p-8d	3.226E-2			3.26E-2	3.330E-2	0.98	
4p-9d	1.965E-2			1.98E-2	2.021E-2	0.98	
4p-10d	1.300E-2			1.31E-2	1.333E-2	0.98	
4d-5p	3.407E-2	3.364E-2		3.34E-2	2.782E-2	1.2	3.77E-2
4d-6p	7.166E-3	6.897E-3		6.89E-3	5.838E-3	1.18	
4d-7p	2.906E-3	2.673E-3		2.66E-3	2.274E-3	1.17	
4d-8p	1.444E-3			1.35E-3	1.155E-3	1.17	
4d-9p	1.038E-3			7.95E-4	6.797E-4	1.17	
4d-10p	5.124E-4			5.14E-4	4.391E-4	1.17	

TABLE III-2 Continued

Lindgard		Guennou	Zhang	Recom	H-like	Recm/H	Fitting
4d-4f	1.582E-3			1.60E-3			2.29E-3
4d-5f	8.862E-1	8.884E-1		8.90E-1	8.903E-1	1	8.86E-1
4d-6f	1.857E-1	1.861E-1		1.86E-1	1.862E-1	1	
4d-7f	7.188E-2	7.231E-2		7.22E-2	7.225E-2	1	
4d-8f	3.643E-2			3.66E-2	3.659E-2	1	
4d-9f	2.134E-2			2.15E-2	2.149E-2	1	
4d-10f	1.377E-2			1.39E-2	1.386E-2	1	
4f-5d	9.001E-3	9.009E-3		9.23E-3	8.871E-3	1.04	9.50E-3
4f-6d	1.573E-3	1.562E-3		1.65E-3	1.583E-3	1.04	
4f-7d	5.613E-4	5.768E-4		5.87E-4	5.644E-4	1.04	
4f-8d	2.550E-4			2.82E-4	2.716E-4	1.04	
4f-9d	1.491E-4			1.60E-4	1.542E-4	1.04	
4f-10d	9.336E-5			1.01E-4	9.713E-5	1.04	
4f-5g	1.340E+0	1.346E+0		1.35E+0	1.346E+0	1	1.35E+0
4f-6g	1.835E-1	1.820E-1		1.82E-1	1.824E-1	1	
4f-7g	5.897E-2	5.856E-2		5.84E-2	5.838E-2	1	
4f-8g	2.698E-2			2.66E-2	2.655E-2	1	
4f-9g	1.482E-2			1.46E-2	1.457E-2	1	
4f-10g	9.165E-3			8.98E-3	8.979E-3	1	
5s-5p	3.298E-1			3.40E-1			3.60E-1
5s-6p	4.448E-1			4.19E-1	6.078E-1	0.69	
5s-7p	1.278E-1	1.225E-1		1.22E-1	1.549E-1	0.79	
5s-8p	5.704E-2			5.46E-2	6.737E-2	0.81	
5s-9p	3.523E-2			2.98E-2	3.675E-2	0.81	
5s-10p	1.946E-2			1.86E-2	2.273E-2	0.82	
5p-6s	1.099E-1			1.10E-1	7.454E-2	1.47	
5p-7s	2.363E-2	2.370E-2		2.36E-2	1.749E-2	1.35	
5p-8s	9.614E-3			9.59E-3	7.268E-3	1.32	
5p-9s	5.066E-3			5.08E-3	3.851E-3	1.32	
5p-10s	3.080E-3			3.08E-3	2.336E-3	1.32	
5p-5d	7.707E-2			7.70E-2			8.46E-2
5p-6d	5.600E-1			5.68E-1	6.247E-1	0.91	
5p-7d	1.472E-1	1.490E-1		1.49E-1	1.570E-1	0.95	
5p-8d	6.417E-2			6.49E-2	6.755E-2	0.96	
5p-9d	3.543E-2			3.51E-2	3.656E-2	0.96	
5p-10d	2.204E-2			2.16E-2	2.249E-2	0.96	
5d-6p	5.901E-2			5.66E-2	4.800E-2	1.18	
5d-7p	1.292E-2	1.200E-2		1.20E-2	1.033E-2	1.16	
5d-8p	5.037E-3			4.74E-3	4.083E-3	1.16	
5d-9p	3.176E-3			2.43E-3	2.094E-3	1.16	
5d-10p	1.490E-3			1.44E-3	1.243E-3	1.16	
5d-5f	3.809E-3			2.50E-3			1.31E-2
5d-6f	8.380E-1			8.44E-1	8.443E-1	1	
5d-7f	1.961E-1	1.963E-1		1.97E-1	1.968E-1	1	

TABLE III-2 Continued

Lindgard		Guennou	Zhang	Recom	H-like	Recm/H	Fitting
5d-8f	8.125E-2			8.08E-2	8.082E-2	1	
5d-9f	4.284E-2			4.24E-2	4.241E-2	1	
5d-10f	2.594E-2			2.55E-2	2.552E-2	1	
5f-6d	2.303E-2			2.40E-2	2.328E-2	1.03	
5f-7d	4.441E-3	4.535E-3		4.56E-3	4.432E-3	1.03	
5f-8d	1.601E-3			1.68E-3	1.630E-3	1.03	
5f-9d	8.330E-4			8.22E-4	7.985E-4	1.03	
5f-10d	4.908E-4			4.73E-4	4.589E-4	1.03	
5f-5g	4.293E-3			4.29E-3			1.79E-3
5f-6g	1.177E+0			1.19E+0	1.185E+0	1	
5f-7g	2.295E-1	2.290E-1		2.29E-1	2.287E-1	1	
5f-8g	8.571E-2			8.45E-2	8.450E-2	1	
5f-9g	4.222E-2			4.15E-2	4.148E-2	1	
5f-10g	2.439E-2			2.39E-2	2.386E-2	1	
5g-6f	7.677E-3			7.38E-3	7.376E-3	1	
5g-7f	1.246E-3	1.241E-3		1.20E-3	1.174E-3	1.02	
5g-8f	4.312E-4			3.97E-4	3.895E-4	1.02	
5g-9f	2.053E-4			1.82E-4	1.787E-4	1.02	
5g-10f	1.164E-4			1.00E-4	9.821E-5	1.02	
5g-6h				1.68E+0	1.676E+0	1	
5g-7h		2.029E-1		2.02E-1	2.018E-1	1	
5g-8h				5.99E-2	5.992E-2	1	
5g-9h				2.59E-2	2.592E-2	1	
5g-10h				1.37E-2	1.375E-2	1	
6s-6p	3.934E-1			4.00E-1			
6s-7p	5.129E-1			5.12E-1	6.736E-1	0.76	
6s-8p	1.418E-1			1.42E-1	1.715E-1	0.83	
6s-9p	7.151E-2			6.21E-2	7.482E-2	0.83	
6s-10p	3.412E-2			3.40E-2	4.099E-2	0.83	
6p-7s	1.405E-1			1.40E-1	9.672E-2	1.45	
6p-8s	3.106E-2			3.10E-2	2.278E-2	1.36	
6p-9s	1.257E-2			1.25E-2	9.498E-3	1.32	
6p-10s	6.548E-3			6.57E-3	5.052E-3	1.3	
6p-6d	1.217E-1			1.20E-1			
6p-7d	5.785E-1			5.80E-1	6.514E-1	0.89	
6p-8d	1.534E-1			1.54E-1	1.658E-1	0.93	
6p-9d	6.830E-2			6.85E-2	7.212E-2	0.95	
6p-10d	3.744E-2			3.74E-2	3.940E-2	0.95	
6d-7p	9.423E-2			8.29E-2	7.024E-2	1.18	
6d-8p	1.990E-2			1.78E-2	1.539E-2	1.16	
6d-9p	9.351E-3			7.12E-3	6.137E-3	1.16	
6d-10p	3.796E-3			3.68E-3	3.170E-3	1.16	
6d-6f	6.444E-4			3.40E-3			
6d-7f	8.359E-1			8.33E-1	8.329E-1	1	

TABLE III-2 Continued

Lindgard		Guennou	Zhang	Recom	H-like	Recm/H	Fitting
6d-8f	2.050E-1			2.04E-1	2.038E-1	1	
6d-9f	8.597E-2			8.62E-2	8.623E-2	1	
6d-10f	4.576E-2			4.62E-2	4.619E-2	1	
6f-7d	4.268E-2			4.22E-2	4.135E-2	1.02	
6f-8d	8.268E-3			8.37E-3	8.205E-3	1.02	
6f-9d	3.155E-3			3.14E-3	3.082E-3	1.02	
6f-10d	1.529E-3			1.56E-3	1.529E-3	1.02	
6f-6g	7.941E-3			7.94E-3			
6f-7g	1.101E+0			1.11E+0	1.110E+0	1	
6f-8g	2.448E-1			2.45E-1	2.453E-1	1	
6f-9g	9.647E-2			9.73E-2	9.733E-2	1	
6f-10g	4.929E-2			4.99E-2	4.990E-2	1	
6g-7f	2.084E-2			2.00E-2	1.981E-2	1.01	
6g-8f	3.581E-3		3.47E-3	3.435E-3	1.01		
6g-9f	1.184E-3			1.20E-3	1.189E-3	1.01	
6g-10f	5.299E-4			5.64E-4	5.588E-4	1.01	
6g-6h							
6g-7h				1.49E+0	1.492E+0	1	
6g-8h				2.66E-1	2.657E-1	1	
6g-9h				9.30E-2	9.304E-2	1	
6g-10h				4.40E-2	4.400E-2	1	
6h-7g				6.29E-3	6.294E-3	1	
6h-8g				9.01E-4	9.010E-4	1	
6h-9g				2.78E-4	2.781E-4	1	
6h-10g				1.21E-4	1.212E-4	1	
6h-7i				2.01E+0	2.008E+0	1	
6h-8i				2.17E-1	2.169E-1	1	
6h-9i				5.98E-2	5.979E-2	1	
6h-10i				2.45E-2	2.455E-2	1	
7s-7p	3.941E-1			4.80E-1			
7s-8p	5.466E-1			5.48E-1	7.407E-1	0.74	
7s-9p	1.755E-1			1.54E-1	1.881E-1	0.82	
7s-10p	6.713E-2			6.73E-2	8.211E-2	0.82	
7p-8s	1.611E-1			1.67E-1	1.192E-1	1.4	
7p-9s	3.561E-2			3.58E-2	2.815E-2	1.27	
7p-10s	1.490E-2			1.49E-2	1.176E-2	1.27	
7p-7d	1.828E-1			1.80E-1			
7p-8d	5.584E-1			5.61E-1	6.843E-1	0.82	
7p-9d	1.555E-1			1.56E-1	1.750E-1	0.89	
7p-10d	7.082E-2			7.12E-2	7.653E-2	0.93	
7d-8p	1.197E-1			1.09E-1	9.385E-2	1.16	
7d-9p	3.087E-2			2.41E-2	2.081E-2	1.16	
7d-10p	9.969E-3			9.69E-3	8.358E-3	1.16	
7d-7f	6.715E-3		4.50E-3				

TABLE III-2 Continued

Lindgard		Guennou	Zhang	Recom	H-like	Recm/H	Fitting
7d-8f	8.302E-1			8.39E-1	8.393E-1	1	
7d-9f	2.092E-1			2.10E-1	2.103E-1	1	
7d-10f	9.139E-2			9.05E-2	9.049E-2	1	
7f-8d	5.944E-2			6.26E-2	6.196E-2	1.01	
7f-9d	1.259E-2			1.28E-2	1.265E-2	1.01	
7f-10d	4.980E-3			4.87E-3	4.824E-3	1.01	
7f-7g	1.123E-2			1.12E-3			
7f-8g	1.060E+0			1.08E+0	1.075E+0	1	
7f-9g	2.533E-1			2.54E-1	2.538E-1	1	
7f-10g	1.061E-1			1.05E-1	1.048E-1	1	
7g-8f	3.647E-2			3.59E-2	3.586E-2	1	
7g-9f	6.760E-3			6.58E-3	6.577E-3	1	
7g-10f	2.529E-3			2.34E-3	2.344E-3	1	
7g-7h							
7g-8h				1.39E+0	1.392E+0	1	
7g-9h				2.91E-1	2.909E-1	1	
7g-10h				1.11E-1	1.110E-1	1	
7h-8g				1.72E-2	1.718E-2	1	
7h-9g				2.73E-3	2.729E-3	1	
7h-10g				8.89E-4	8.889E-4	1	
7h-7i							
7h-8i				1.81E+0	1.806E+0	1	
7h-9i				2.98E-1	2.977E-1	1	
7h-10i				9.87E-2	9.866E-2	1	
7i-8h				5.48E-3	5.482E-3	1	
7i-9h				7.12E-4	7.118E-4	1	
7i-10h				2.05E-4	2.048E-4	1	
7i-8k				2.34E+0	2.340E+0	1	
7i-9k				2.29E-1	2.289E-1	1	
7i-10k				5.88E-2	5.876E-2	1	
8s-8p	4.664E-1			5.40E-1			
8s-9p	7.454E-1			5.98E-1	8.086E-1	0.74	
8s-10p	1.587E-1			1.66E-1	2.047E-1	0.81	
8p-9s	1.962E-1			1.96E-1	1.420E-1	1.38	
8p-10s	4.285E-2			4.30E-2	3.357E-2	1.28	
8p-8d	2.319E-1			2.30E-1			
8p-9d	6.082E-1			6.06E-1	7.210E-1	0.84	
8p-10d	1.638E-1			1.64E-1	1.846E-1	0.89	
8d-9p	1.974E-1			1.37E-1	1.184E-1	1.16	
8d-10p	3.196E-2			3.07E-2	2.649E-2	1.16	
8d-8f	9.854E-3			5.40E-3			
8d-9f	8.688E-1			8.56E-1	8.558E-1	1	
8d-10f	2.168E-1			2.17E-1	2.171E-1	1	
8f-9d	8.612E-2			8.44E-2	8.439E-2	1	

TABLE III-2 Continued

Lindgard		Guennou	Zhang	Recom	H-like	Recm/H	Fitting
8f-10d	1.749E-2			1.76E-2	1.760E-2	1	
8f-8g	1.428E-2			1.43E-2			
8f-9g	1.051E+0			1.06E+0	1.063E+0	1	
8f-10g	2.561E-1			2.60E-1	2.601E-1	1	
8g-9f	5.684E-2			5.46E-2	5.461E-2	1	
8g-10f	1.038E-2			1.04E-2	1.042E-2	1	
8g-8h							
8g-9h				1.34E+0	1.337E+0	1	
8g-10h				3.03E-1	3.031E-1	1	
8h-9g				3.15E-2	3.153E-2	1	
8h-10g				5.37E-3	5.366E-3	1	
8h-8i							
8h-9i				1.69E+0	1.685E+0	1	
8h-10i				3.33E-1	3.328E-1	1	
8i-9h				1.51E-2	1.514E-2	1	
8i-10h				2.22E-3	2.217E-3	1	
8i-8k							
8i-9k				2.12E+0	2.124E+0	1	
8i-10k				3.25E-1	3.253E-1	1	
8k-9i				4.85E-3	4.853E-3	1	
8k-10i				5.76E-4	5.759E-4	1	
8k-9l				2.67E+0	2.672E+0	1	
8k-10l				2.39E-1	2.387E-1	1	
9s-9p	1.566E-1			6.00E-1			
9s-10p	6.153E-1			6.49E-1	8.770E-1	0.74	
9p-10s	1.804E-1			2.26E-1	1.649E-1	1.37	
9p-9d	4.785E-1			2.80E-1			
9p-10d	5.162E-1			6.08E-1	7.600E-1	0.8	
9d-10p	1.746E-1			1.67E-1	1.437E-1	1.16	
9d-9f	6.348E-3			6.40E-3			
9d-10f	8.738E-1			8.79E-1	8.788E-1	1	
9f-10d	1.089E-1			1.08E-1	1.082E-1	1	
9f-9g	1.720E-2			1.72E-2			
9f-10g	1.052E+0			1.07E+0	1.065E+0	1	
9g-10f	7.793E-2			7.54E-2	7.540E-2	1	
9g-9h							
9g-10h				1.31E+0	1.308E+0	1	
9h-10g				4.86E-2	4.858E-2	1	
9h-9i							
9h-10i				1.61E+0	1.611E+0	1	
9i-10h				2.81E-2	2.808E-2	1	
9i-9k							
9i-10k				1.99E+0	1.986E+0	1	
9k-10i				1.35E-2	1.353E-2	1	

TABLE III-2 Continued

Lindgard	Guennou	Zhang	Recom	H-like	Recm/H	Fitting
9k-9l						
9k-10l			2.44E+0	2.445E+0	1	
9l-10k			4.35E-3	4.351E-3	1	
9l-10m			3.01E+0	3.005E+0	1	
10s-10p	6.725E-1			6.73E-1		
10p-10d	2.103E-1			2.10E-1		
10d-10f	7.163E-3			7.16E-3		
10f-10g	1.999E-2			2.00E-2		

TABLE III-3

	A	D	c1	c2	c3	a
2s-2p	7.640723D-1	5.310492D-1	2.991032D+0	0.000000D+0	0.000000D+0	1.196063D+0
2s-3s	0.000000D+0	7.918746D-2	-2.910180D-2	0.000000D+0	0.000000D+0	7.393565D-1
2s-3p	1.440175D-1	-1.196448D-1	2.173784D-1	0.000000D+0	0.000000D+0	3.889709D-1
2s-3d	0.000000D+0	2.163340D-1	0.000000D+0	-2.793427D+0	5.321434D+0	2.461027D+0
2s-4s	0.000000D+0	1.596202D-2	-7.177122D-3	0.000000D+0	0.000000D+0	1.083560D+0
2s-4p	2.630670D-2	-6.741304D-3	0.000000D+0	5.023527D-2	0.000000D+0	7.227175D-1
2s-4d	0.000000D+0	3.746392D-2	-5.770201D-2	5.495608D-2	0.000000D+0	6.727817D-1
2s-4f	0.000000D+0	1.174261D-2	-9.108478D-3	7.568071D-3	0.000000D+0	-3.915886D-2
2s-5s	0.000000D+0	6.255148D-3	-4.220619D-3	0.000000D+0	0.000000D+0	1.974137D+0
2s-5p	9.867846D-3	-1.164876D-3	0.000000D+0	1.175748D-2	0.000000D+0	4.439751D-1
2s-5d	0.000000D+0	1.140576D-2	0.000000D+0	-7.342349D-2	1.384785D-1	1.290458D+0
2s-5f	0.000000D+0	6.091137D-3	-4.259790D-3	3.617222D-3	0.000000D+0	-1.331978D-1
2s-5g	0.000000D+0	3.617774D-4	-4.121904D-4	5.181118D-4	0.000000D+0	-2.232748D-1
2p-3s	2.218891D-2	3.055179D-3	-9.085581D-2	3.094587D-1	0.000000D+0	1.575547D+0
2p-3p	0.000000D+0	2.613280D-1	3.243618D-3	0.000000D+0	0.000000D+0	-7.875924D-1
2p-3d	8.449319D-1	1.545997D-1	0.000000D+0	2.293689D+0	0.000000D+0	9.401568D-1
2p-4s	6.480121D-3	-6.476109D-3	1.318082D-2	0.000000D+0	0.000000D+0	1.885144D-1
2p-4p	0.000000D+0	5.795864D-2	-4.379748D-2	9.151233D-2	0.000000D+0	6.995491D-1
2p-4d	1.424997D-1	3.471565D-2	1.138988D-1	0.000000D+0	0.000000D+0	-1.078126D-1
2p-4f	0.000000D+0	6.128786D-2	-1.140040D-1	1.005270D-1	0.000000D+0	2.971643D-1
2p-5s	8.792720D-4	1.546248D-3	0.000000D+0	-3.859788D-2	1.184347D-1	1.735203D+0
2p-5p	0.000000D+0	2.064527D-2	0.000000D+0	-3.237300D-2	1.086304D-1	9.613138D-1
2p-5d	4.202092D-2	3.771562D-2	0.000000D+0	-7.553372D-3	1.223771D-1	5.856968D-1
2p-5f	0.000000D+0	2.702234D-2	0.000000D+0	-2.002802D-1	3.264976D-1	8.781868D-1
2p-5g	0.000000D+0	1.146796D-3	0.000000D+0	-3.494549D-3	5.563086D-3	1.901819D-1

TABLE III-4

	A	D	c1	c2	a
1s-2s	0.000D+0	4.439D-1	-2.198D-1	4.500D-5	1.670D+0
1s-2p	2.220D+0	6.593D-1	-3.058D+0	9.199D+0	0.970D+0
1s-3s	0.000D+0	8.814D-2	-4.442D-2	4.206D-2	0.680D+0
1s-3p	3.560D-1	2.292D-1	-6.011D-1	1.250D+0	0.680D+0
1s-3d	0.000D+0	7.443D-2	-1.382D-1	1.221D-1	0.050D+0
1s-4s	0.000D+0	3.278D-2	-1.687D-2	1.775D-2	0.590D+0
1s-4p	1.237D-1	9.396D-2	-2.191D-1	4.119D-1	0.580D+0
1s-4d	0.000D+0	3.528D-2	-6.354D-2	5.583D-2	0.000D+0
1s-4f	0.000D+0	5.641D-4	-7.781D-4	1.030D-3	-0.350D+0
1s-5s	0.000D+0	1.585D-2	-8.095D-3	8.751D-3	0.530D+0
1s-5p	5.808D-2	4.720D-2	-1.054D-1	1.904D-1	0.540D+0
1s-5d	0.000D+0	1.858D-2	-3.292D-2	2.892D-2	-0.020D+0
1s-5f	0.000D+0	4.312D-4	-5.896D-4	7.834D-4	-0.360D+0
1s-5g	0.000D+0	6.487D-6	-1.799D-5	2.156D-5	-0.410D+0
2s-3s	0.000D+0	5.316D+0	-1.898D-1	-8.470D+0	2.100D+0
2s-3p	1.252D+1	-5.942D+0	-1.614D+1	1.425D+2	2.030D+0
2s-3d	0.000D+0	1.679D+1	4.972D+1	-1.314D+3	9.130D+0
2s-4s	0.000D+0	1.036D+0	-1.023D-2	-1.697D+0	2.180D+0
2s-4p	2.192D+0	-2.039D-1	-3.458D+0	1.810D+1	1.690D+0
2s-4d	0.000D+0	2.223D+0	-2.620D+0	2.373D+0	0.410D+0
2s-4f	0.000D+0	1.133D+0	-7.158D-1	5.573D-1	-0.070D+0
2s-5s	0.000D+0	3.980D-1	-8.900D-2	2.995D-2	-0.250D+0
2s-5p	7.987D-1	3.660D-2	-1.121D+0	4.906D+0	1.400D+0
2s-5d	0.000D+0	7.195D-1	-7.755D-1	7.817D-1	0.260D+0
2s-5f	0.000D+0	5.359D-1	-3.499D-1	3.139D-1	-0.080D+0
2s-5g	0.000D+0	4.835D-2	-6.707D-2	8.642D-2	-0.070D+0
2p-3s	1.174D+0	-4.617D-1	-2.643D+0	1.719D+1	1.700D+0
2p-3p	0.000D+0	1.797D+1	-9.936D+0	1.722D+1	1.030D+0
2p-3d	6.012D+1	1.445D+1	-1.217D+2	7.103D+2	1.970D+0
2p-4s	1.949D-1	4.415D-2	-5.424D-1	2.121D+0	0.980D+0
2p-4p	0.000D+0	3.500D+0	-1.711D+0	3.577D+0	0.460D+0
2p-4d	7.795D+0	7.078D+0	-1.335D+1	4.229D+1	1.010D+0
2p-4f	0.000D+0	5.329D+0	-1.237D+1	1.285D+1	0.620D+0
2p-5s	6.933D-2	3.655D-2	-2.188D-1	7.228D-1	0.750D+0
2p-5p	0.000D+0	1.333D+0	-6.459D-1	1.402D+0	0.300D+0
2p-5d	2.535D+0	3.108D+0	-4.862D+0	1.214D+1	0.750D+0
2p-5f	0.000D+0	2.552D+0	-5.179D+0	5.010D+0	0.370D+0
2p-5g	0.000D+0	1.245D-1	-1.350D-1	1.375D-1	-0.210D+0
3s-4s	0.000D+0	2.289D+1	3.609D+0	-5.230D+1	2.570D+0
3s-4p	3.988D+1	-3.700D+1	6.100D+0	4.086D+2	2.030D+0
3s-4d	0.000D+0	5.656D+1	-1.997D+2	3.127D+1	4.710D+0
3s-4f	0.000D+0	2.486D+1	-5.293D+1	1.680D+2	4.710D+0
3s-5s	0.000D+0	4.240D+0	6.948D-1	-7.022D+0	2.000D+0
3s-5p	6.808D+0	-2.820D+0	-1.222D+1	8.263D+1	2.030D+0

TABLE III-4 Continued

	A	D	c1	c2	a
3s-5d	0.000D+0	8.516D+0	-1.625D+1	1.377D+1	1.850D+0
3s-5f	0.000D+0	2.167D+0	-4.641D+0	9.895D+0	0.940D+0
3s-5g	0.000D+0	5.040D+0	-9.101D+0	1.319D+1	0.900D+0
3p-4s	7.961D+0	-6.466D+0	-1.051D+1	1.283D+2	2.180D+0
3p-4p	0.000D+0	8.431D+1	-4.742D+1	2.063D+0	2.080D+0
3p-4d	1.526D+2	-6.928D+1	-2.135D+2	2.548D+3	2.440D+0
3p-4f	0.000D+0	1.853D+2	-5.579D+2	4.526D+2	3.970D+0
3p-5s	1.254D+0	-3.187D-1	-1.699D+0	9.670D+0	1.220D+0
3p-5p	0.000D+0	1.584D+1	-6.889D+0	5.954D+0	0.980D+0
3p-5d	2.350D+1	3.721D+0	-5.683D+1	3.373D+2	2.180D+0
3p-5f	0.000D+0	1.357D+1	-1.386D+1	1.689D+1	0.460D+0
3p-5g	0.000D+0	1.859D+1	-1.156D+1	8.202D+0	0.130D+0
3d-4s	0.000D+0	3.302D+0	-1.484D+1	4.786D+1	2.870D+0
3d-4p	4.522D+0	2.624D+0	-1.561D+1	1.045D+2	1.700D+0
3d-4d	0.000D+0	1.119D+2	-3.648D+1	9.376D+1	1.230D+0
3d-4f	4.186D+2	3.280D+1	-6.693D+2	6.589D+3	2.340D+0
3d-5s	0.000D+0	7.412D-1	-1.965D+0	5.230D+0	1.150D+0
3d-5p	6.216D-1	1.752D+0	-4.534D+0	1.617D+1	0.820D+0
3d-5d	0.000D+0	2.029D+1	-6.422D+0	2.108D+1	0.520D+0
3d-5f	4.405D+1	4.932D+1	-1.368D+2	5.931D+2	1.840D+0
3d-5g	0.000D+0	5.708D+1	-1.862D+2	2.504D+2	1.770D+0
4s-5s	0.000D+0	6.612D+1	1.000D+1	-1.663D+2	3.030D+0
4s-5p	9.674D+1	-1.321D+2	2.874D+2	-5.845D+0	0.880D+0
4s-5d	0.000D+0	1.300D+2	-5.892D+2	8.738D+2	4.100D+0
4s-5f	0.000D+0	5.742D+1	-3.663D+1	9.020D+0	2.610D+0
4s-5g	0.000D+0	3.089D+1	-6.282D+1	1.094D+2	1.990D+0
4p-5s	2.822D+1	-3.757D+1	7.376D+1	1.018D+2	1.510D+0
4p-5p	0.000D+0	2.447D+2	-1.367D+2	9.887D+0	1.950D+0
4p-5d	3.250D+2	-2.768D+2	-4.193D+1	4.974D+3	2.430D+0
4p-5f	0.000D+0	4.383D+2	-2.045D+3	2.024D+2	7.010D+0
4p-5g	0.000D+0	1.507D+2	-5.657D+2	2.931D+3	7.710D+0
4d-5s	0.000D+0	1.565D+1	-7.361D+1	1.766D+2	4.070D+0
4d-5p	2.473D+1	-6.805D+0	-2.958D+1	4.499D+2	2.270D+0
4d-5d	0.000D+0	3.751D+2	-1.765D+2	2.539D+1	3.350D+0
4d-5f	7.913D+2	-3.773D+2	-1.524D+3	1.884D+4	2.810D+0
4d-5g	0.000D+0	7.780D+2	-2.661D+3	3.690D+3	3.970D+0
4f-5s	0.000D+0	2.614D+0	-1.070D+1	4.822D+1	2.550D+0
4f-5p	0.000D+0	1.289D+1	-4.915D+1	1.914D+2	2.420D+0
4f-5d	1.104D+1	1.540D+1	-4.549D+1	3.197D+2	1.740D+0
4f-5f	0.000D+0	4.009D+2	-1.054D+2	3.443D+2	1.680D+0
4f-5g	1.675D+3	-1.253D+1	-3.772D+3	4.307D+4	2.930D+0

TABLE III-5

	A	D	c
1, 2	0.222E+1	0.873E+0	0.186E+1
1, 3	0.356E+0	0.349E+0	0.354E+0
1, 4	0.124E+0	0.148E+0	0.130E+0
1, 5	0.581E-1	0.753E-1	0.624E-1
1, 6	0.321E-1	0.434E-1	0.349E-1
1, 7	0.197E-1	0.272E-1	0.216E-1
1, 8	0.129E-1	0.182E-1	0.143E-1
1, 9	0.898E-2	0.128E-1	0.993E-2
1,10	0.649E-2	0.930E-2	0.719E-2
2, 3	0.738E+2	0.345E+2	0.919E+2
2, 4	0.102E+2	0.179E+2	0.171E+2
2, 5	0.340E+1	0.820E+1	0.640E+1
2, 6	0.159E+1	0.442E+1	0.317E+1
2, 7	0.885E+0	0.266E+1	0.182E+1
2, 8	0.549E+0	0.173E+1	0.115E+1
2, 9	0.366E+0	0.119E+1	0.778E+0
2,10	0.257E+0	0.853E+0	0.552E+0
3, 4	0.624E+3	0.253E+3	0.917E+3
3, 5	0.762E+2	0.167E+3	0.164E+3
3, 6	0.241E+2	0.785E+2	0.608E+2
3, 7	0.110E+2	0.432E+2	0.301E+2
3, 8	0.605E+1	0.265E+2	0.175E+2
3, 9	0.373E+1	0.175E+2	0.111E+2
3,10	0.249E+1	0.123E+2	0.760E+1
4, 5	0.295E+4	0.837E+3	0.476E+4
4, 6	0.330E+3	0.792E+3	0.822E+3
4, 7	0.996E+2	0.381E+3	0.300E+3
4, 8	0.441E+2	0.212E+3	0.148E+3
4, 9	0.239E+2	0.132E+3	0.858E+2
4,10	0.146E+2	0.879E+2	0.549E+2
5, 6	0.101E+5	0.162E+4	0.172E+5
5, 7	0.106E+4	0.264E+4	0.290E+4
5, 8	0.306E+3	0.129E+4	0.104E+4
5, 9	0.132E+3	0.722E+3	0.510E+3
5,10	0.701E+2	0.450E+3	0.295E+3
6, 7	0.278E+5	0.109E+4	0.496E+5
6, 8	0.277E+4	0.684E+4	0.815E+4
6, 9	0.776E+3	0.339E+4	0.290E+4
6,10	0.327E+3	0.191E+4	0.141E+4
7, 8	0.662E+5	-.355E+4	0.122E+6
7, 9	0.634E+4	0.154E+5	0.196E+5
7,10	0.173E+4	0.770E+4	0.690E+4
8, 9	0.141E+6	-.181E+5	0.265E+6
8,10	0.131E+5	0.309E+5	0.422E+5
9,10	0.276E+6	-.508E+5	0.529E+6

Figure Captions

Fig. III-1 Excitation cross sections for the transitions of 2s-3s, 2s-3d and 2s-3d. (a); hydrogenic approximation. (b); the data described in section D-1.

Fig. IV-1 Excited level population and amplification gain by use of atomic data in section III for T_e=20eV.

Fig. IV-2 The same with Fig. IV-1 for T_e=30eV.

Fig. IV-3 The same with Fig. IV-1 for T_e=50eV.

Fig. IV-4 The amplification gain with *l*-changing process are compared with that without *l*-changing process. Electron temperature is 30eV.

Fig. IV-5 The same with Fig. IV-4. Electron temperature is 50eV.

Fig. IV-6 Excited level population and amplification gain by use of atomic data in section II for T_e=20eV.

Fig. IV-7 The same with Fig. IV-4 for T_e=30eV.

Fig. IV-8 The same with Fig. IV-4 for T_e=50eV.

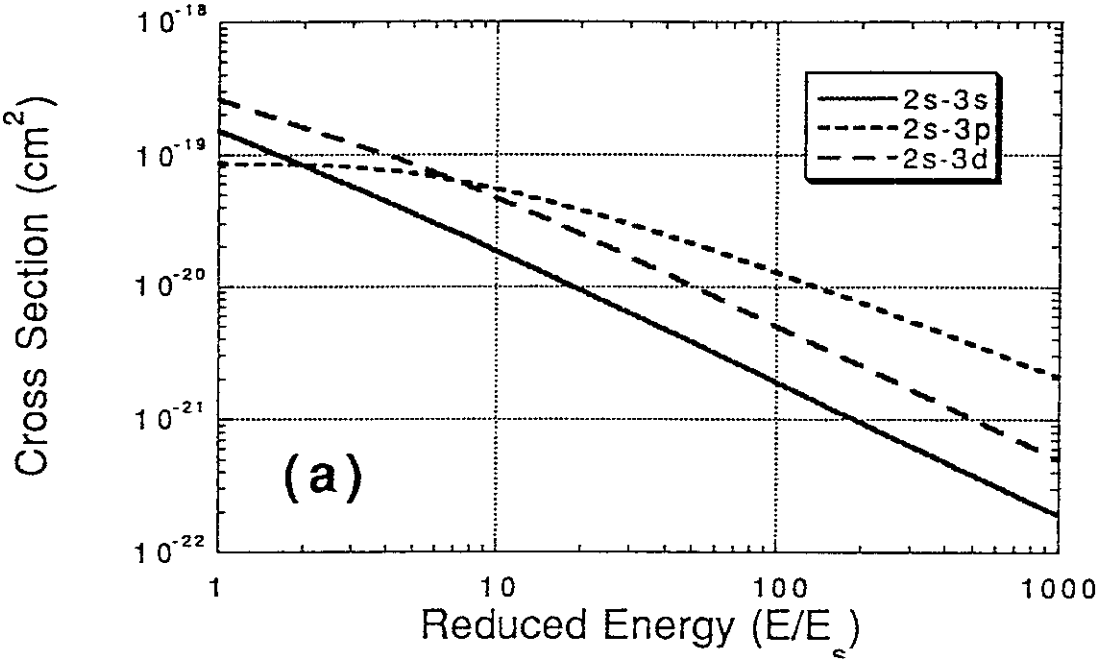

Fig. III-1 (a)

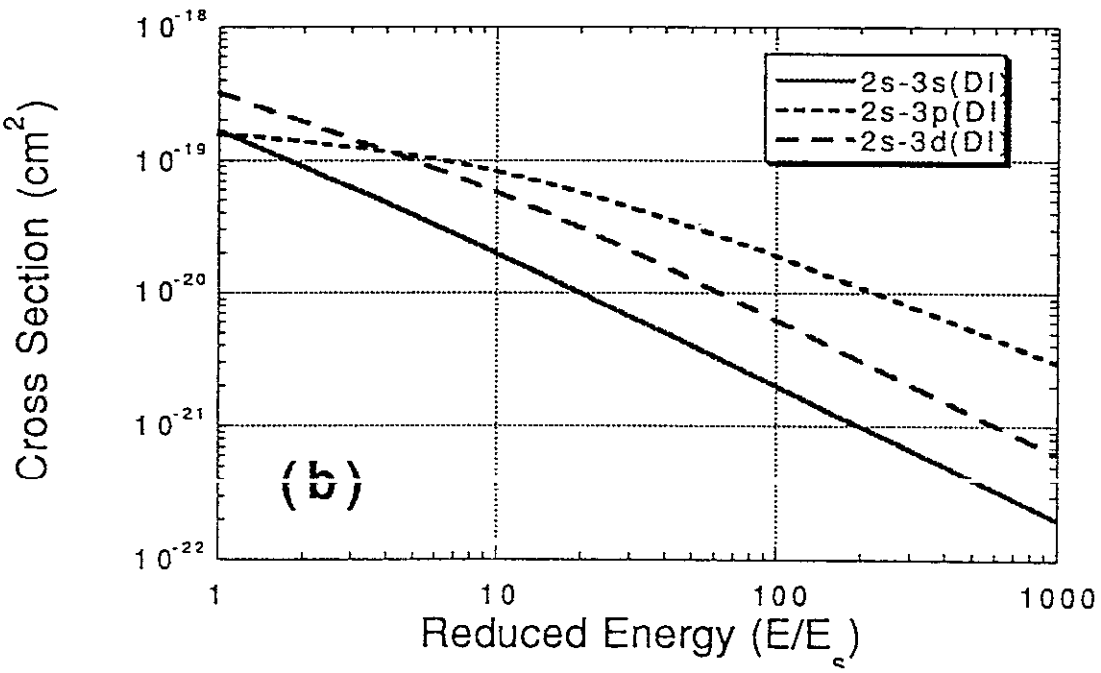

Fig. III-1 (b)

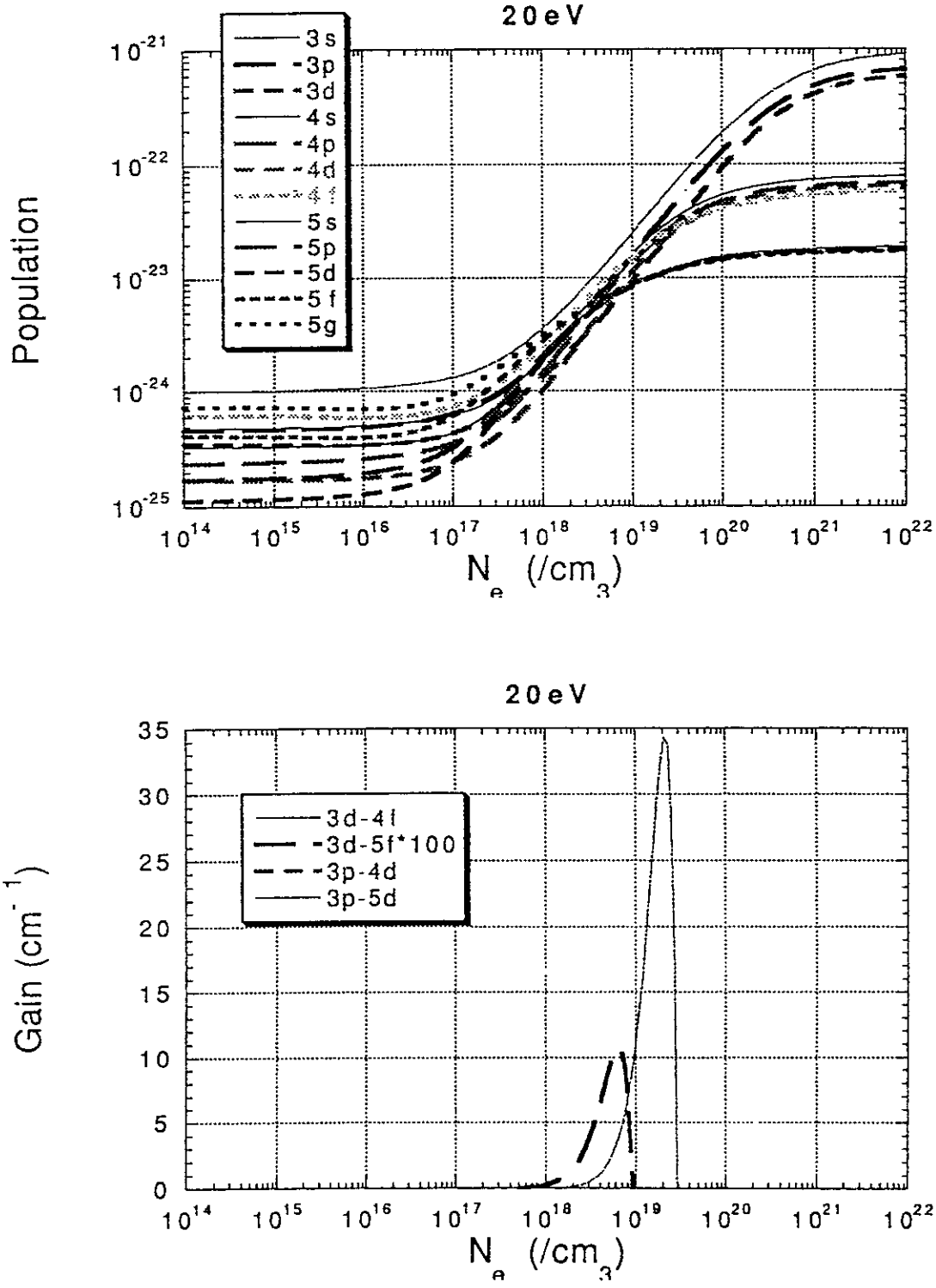
20eV
Population
3s
3p
3d
4s
4p
4d
4f
5s
5p
5d
5f
5g
10^{-21}
10^{-22}
10^{-23}
10^{-24}
10^{-25}
10^{14} 10^{15} 10^{16} 10^{17} 10^{18} 10^{19} 10^{20} 10^{21} 10^{22}
N_e (/cm_3)
20eV
Gain (cm^{-1})
3d-4f
3d-5f*100
3p-4d
3p-5d
35
30
25
20
15
10
5
0
10^{14} 10^{15} 10^{16} 10^{17} 10^{18} 10^{19} 10^{20} 10^{21} 10^{22}
N_e (/cm_3)

Fig. IV-1

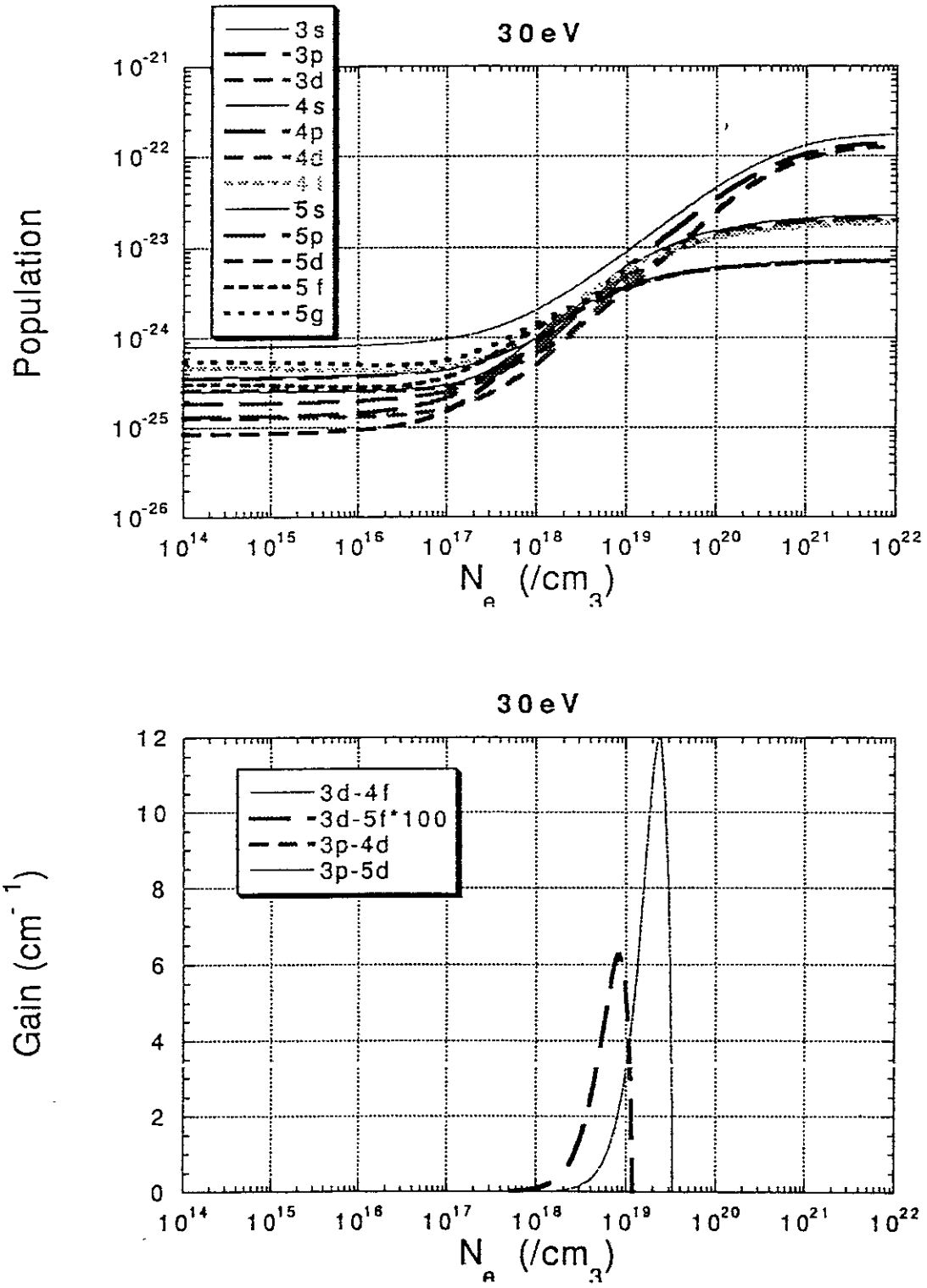
30eV
3s
3p
3d
4s
4p
4d
4f
5s
5p
5d
5f
5g
Population
10^{-21}
10^{-22}
10^{-23}
10^{-24}
10^{-25}
10^{-26}
10^{14} 10^{15} 10^{16} 10^{17} 10^{18} 10^{19} 10^{20} 10^{21} 10^{22}
N_e (/cm$_3$)
30eV
3d-4f
3d-5f*100
3p-4d
3p-5d
Gain (cm^{-1})
12
10
8
6
4
2
0
10^{14} 10^{15} 10^{16} 10^{17} 10^{18} 10^{19} 10^{20} 10^{21} 10^{22}
N_e (/cm$_3$)

Fig. IV-2

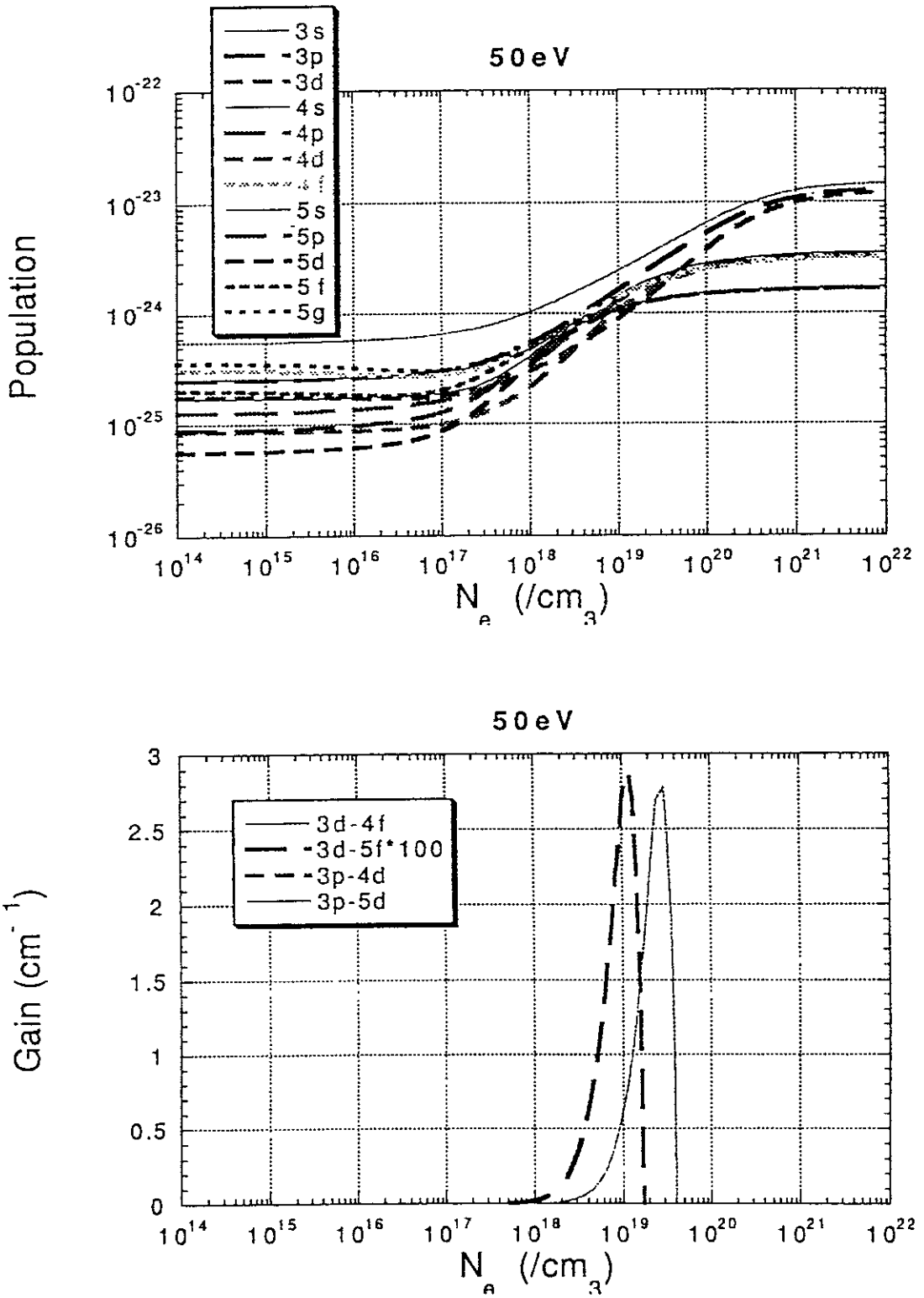
50eV
3s
3p
3d
4s
4p
4d
4f
5s
5p
5d
5f
5g
Population
10^{-22}
10^{-23}
10^{-24}
10^{-25}
10^{-26}
10^{14} 10^{15} 10^{16} 10^{17} 10^{18} 10^{19} 10^{20} 10^{21} 10^{22}
N_e (/cm$_3$)
50eV
3d-4f
3d-5f*100
3p-4d
3p-5d
Gain (cm^{-1})
3
2.5
2
1.5
1
0.5
0
10^{14} 10^{15} 10^{16} 10^{17} 10^{18} 10^{19} 10^{20} 10^{21} 10^{22}
N_e (/cm$_3$)

Fig. IV-3

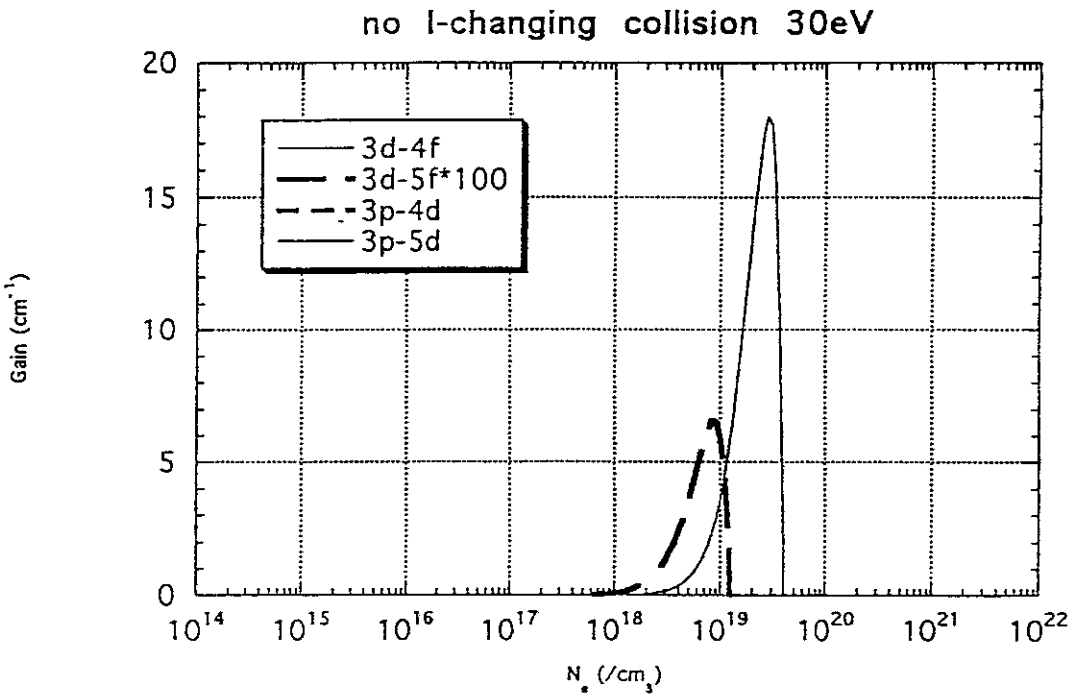
no l-changing collision 30eV
Gain (cm^{-1})
20
15
10
5
0
3d-4f
3d-5f*100
3p-4d
3p-5d
10^{14} 10^{15} 10^{16} 10^{17} 10^{18} 10^{19} 10^{20} 10^{21} 10^{22}
N_e (/cm$_3$)

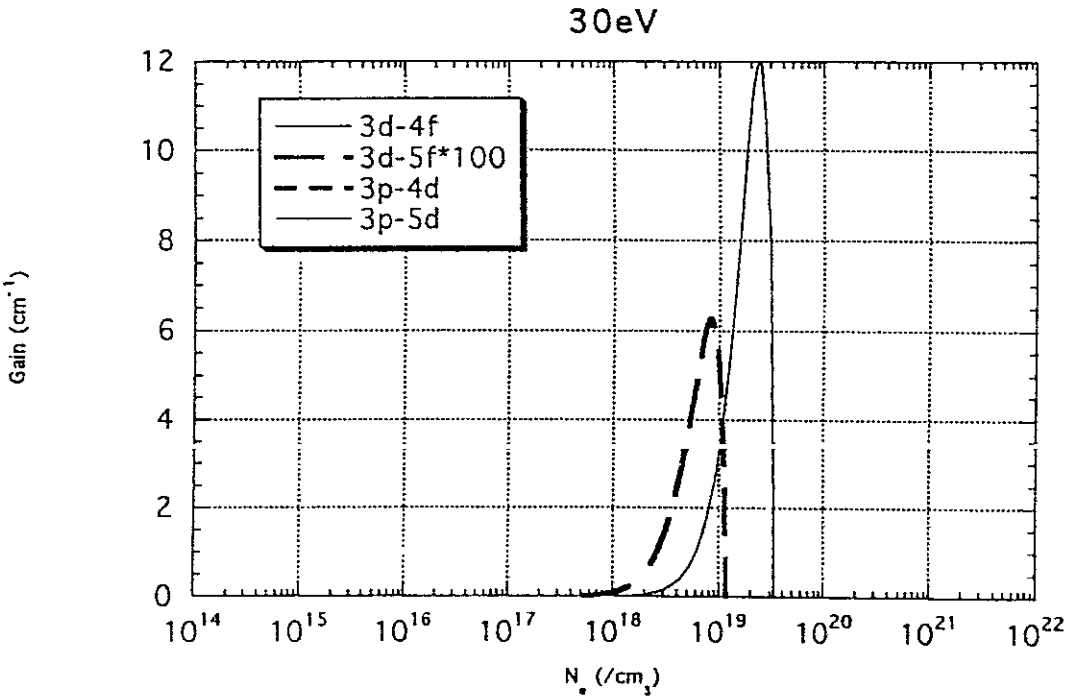
30eV
Gain (cm^{-1})
12
10
8
6
4
2
0
3d-4f
3d-5f*100
3p-4d
3p-5d
10^{14} 10^{15} 10^{16} 10^{17} 10^{18} 10^{19} 10^{20} 10^{21} 10^{22}
N_e (/cm$_3$)

Fig. IV-4

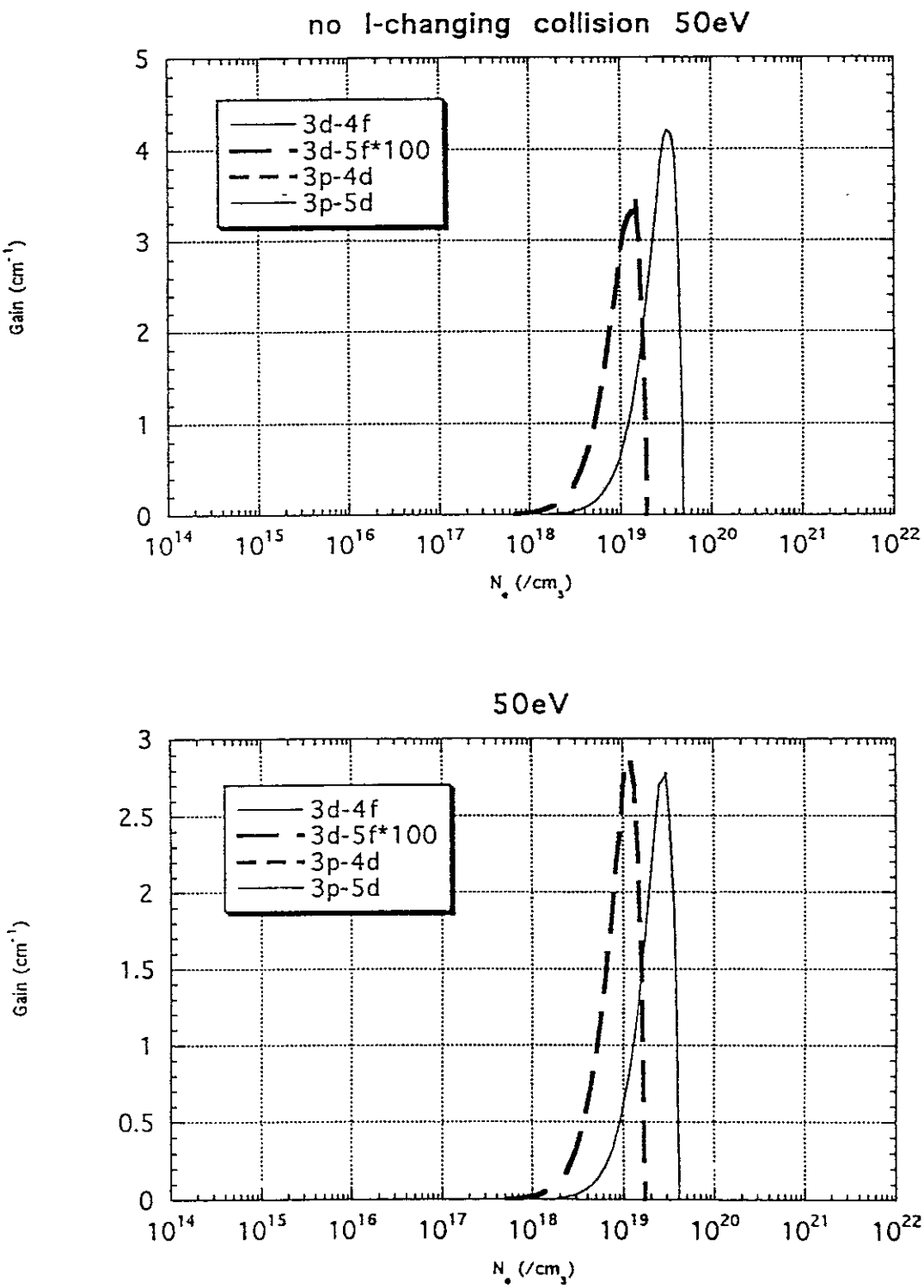
no l-changing collision 50eV
3d-4f
-3d-5f*100
-3p-4d
3p-5d
Gain (cm^{-1})
N$_e$ (/cm$_3$)
50eV
3d-4f
-3d-5f*100
-3p-4d
3p-5d
Gain (cm^{-1})
N$_e$ (/cm$_3$)

Fig. IV-5

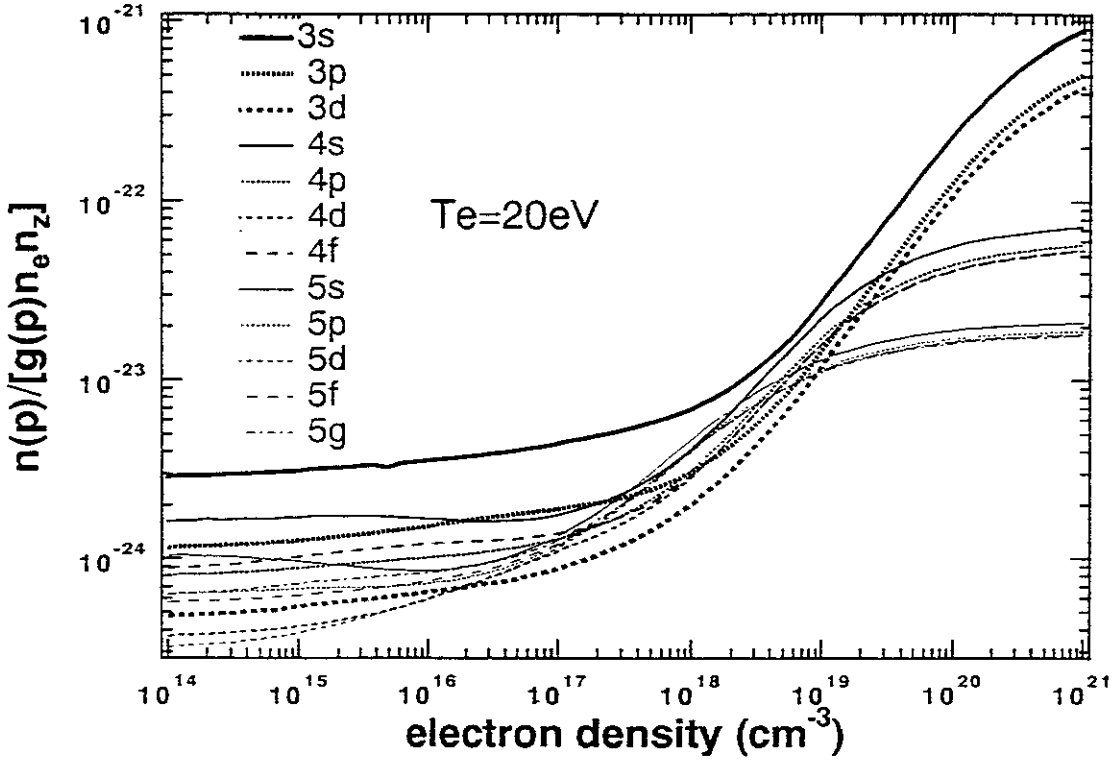
3s
3p
3d
4s
4p
4d
4f
5s
5p
5d
5f
5g
Te=20eV
n(p)/[g(p)n_e n_z]
electron density (cm^-3)

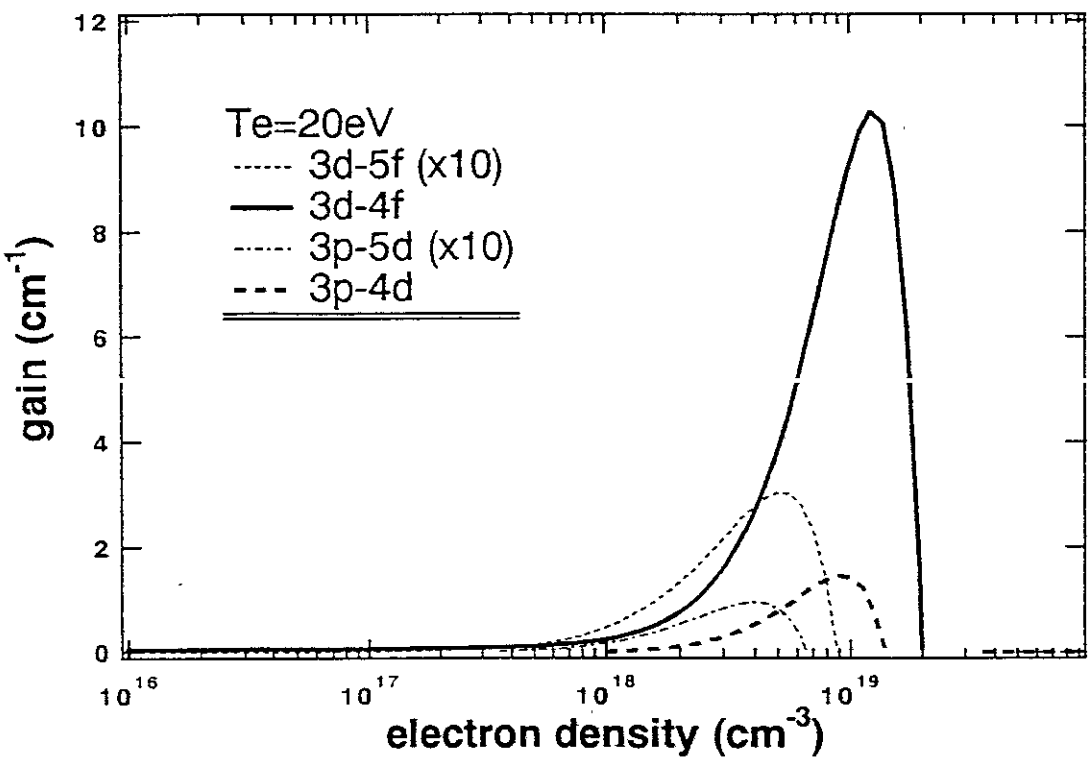
Te=20eV
3d-5f (x10)
3d-4f
3p-5d (x10)
3p-4d
gain (cm^-1)
electron density (cm^-3)

Fig. IV-6

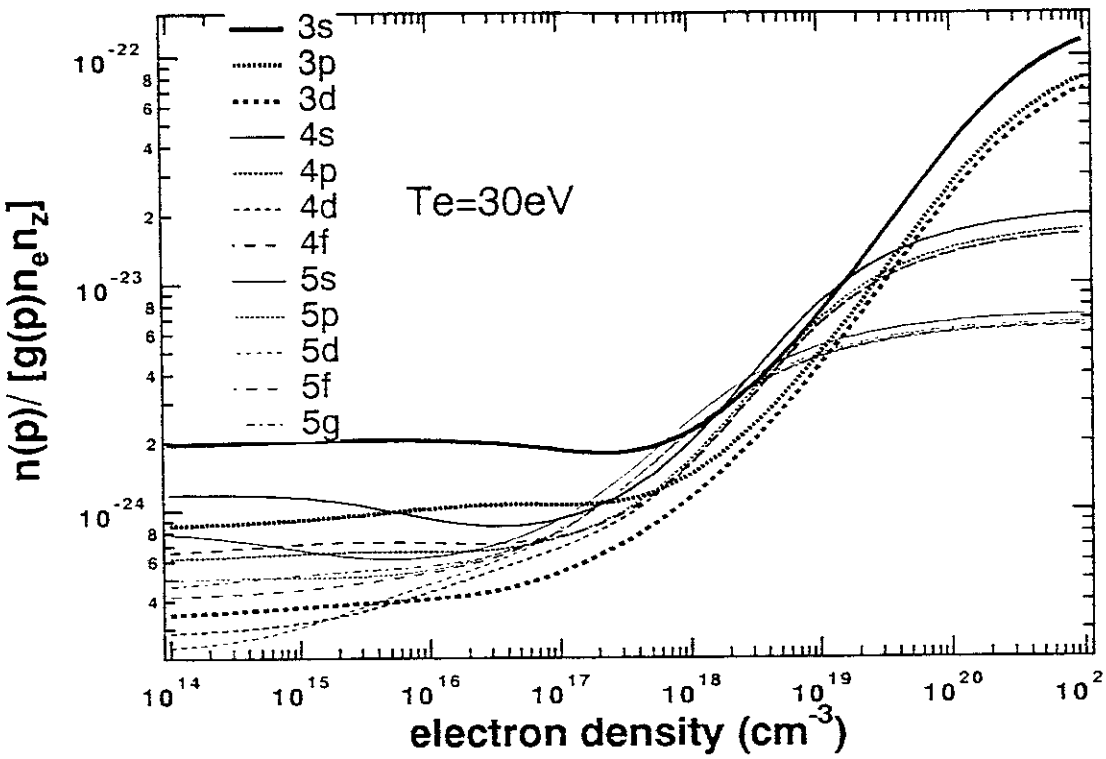
3s
3p
3d
4s
4p
4d
4f
5s
5p
5d
5f
5g
Te=30eV
n(p)/ [g(p)n_e n_z]
electron density (cm^-3)

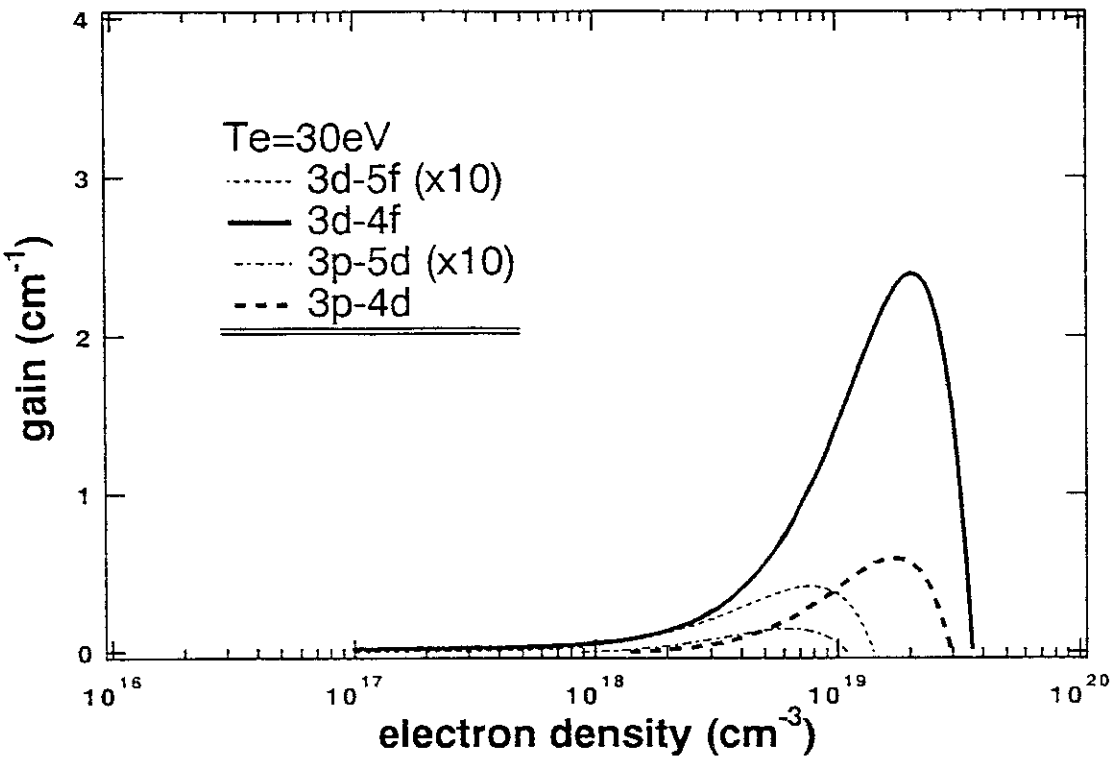
Te=30eV
3d-5f (x10)
3d-4f
3p-5d (x10)
3p-4d
gain (cm^-1)
electron density (cm^-3)

Fig. IV-7

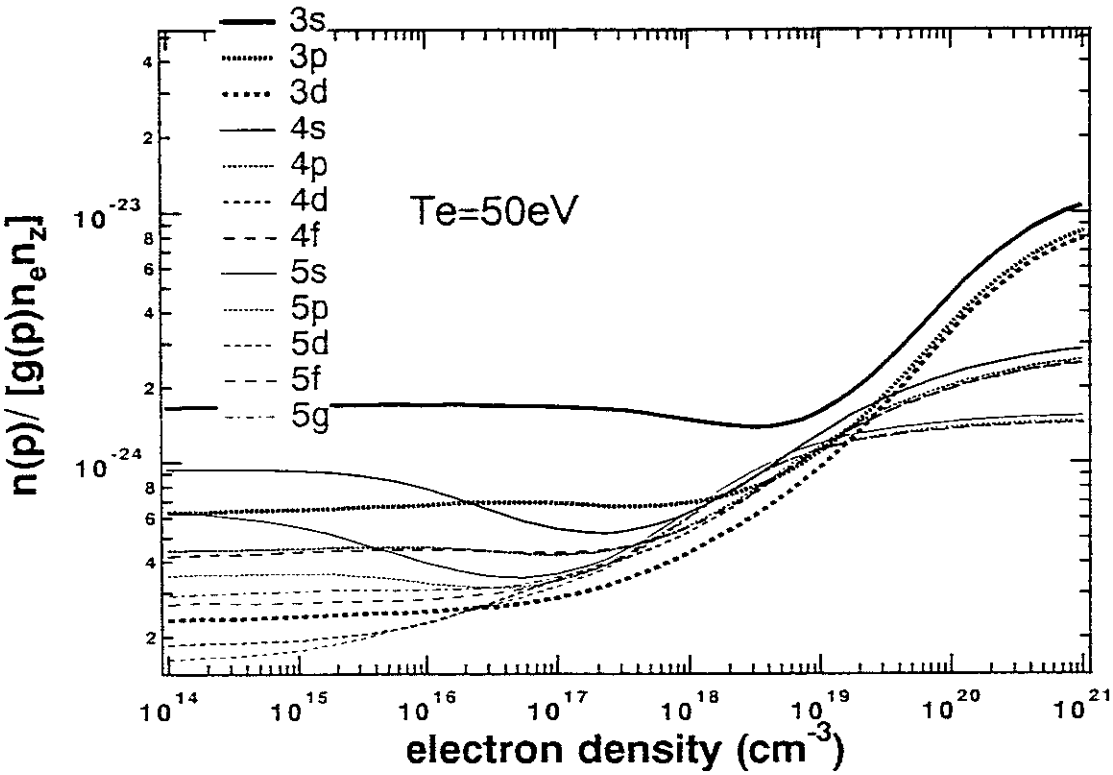
3s
3p
3d
4s
4p
4d
4f
5s
5p
5d
5f
5g
Te=50eV
n(p)/ [g(p)n_e n_z]
electron density (cm^-3)

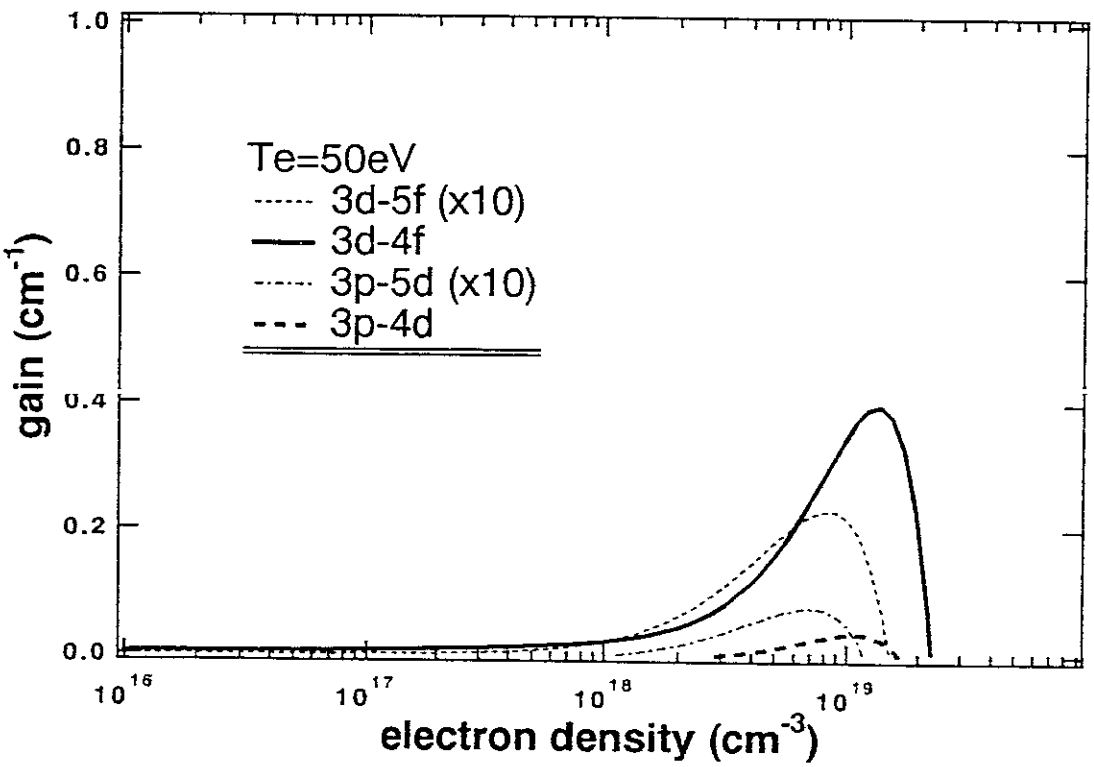
Te=50eV
3d-5f (x10)
3d-4f
3p-5d (x10)
3p-4d
gain (cm^-1)
electron density (cm^-3)

Fig. IV-8

Publication List of NIFS-DATA Series

NIFS-DATA-1 Y. Yamamura, T. Takiguchi and H. Tawara,
Data Compilation of Angular Distributions of Sputtered Atoms; Jan. 1990

NIFS-DATA-2 T. Kato, J. Lang and K. E. Berrington,
Intensity Ratios of Emission Lines from OV Ions for Temperature and Density Diagnostics ; Mar. 1990 [At Data and Nucl Data Tables 44(1990)133]

NIFS-DATA-3 T. Kaneko,
Partial Electronic Straggling Cross Sections of Atoms for Protons ;Mar. 1990

NIFS-DATA-4 T. Fujimoto, K. Sawada and K. Takahata,
Cross Section for Production of Excited Hydrogen Atoms Following Dissociative Excitation of Molecular Hydrogen by Electron Impact ; Mar. 1990

NIFS-DATA-5 H. Tawara,
Some Electron Detachment Data for H^- Ions in Collisions with Electrons, Ions, Atoms and Molecules –an Alternative Approach to High Energy Neutral Beam Production for Plasma Heating–; Apr. 1990

NIFS-DATA-6 H. Tawara, Y. Itikawa, H. Nishimura, H. Tanaka and Y. Nakamura,
Collision Data Involving Hydro-Carbon Molecules; July 1990 [Supplement to Nucl. Fusion 2(1992)25]

NIFS-DATA-7 H.Tawara,
Bibliography on Electron Transfer Processes in Ion-Ion/Atom/Molecule Collisions –Updated 1990–; Aug. 1990

NIFS-DATA-8 U.I.Safronova, T.Kato, K.Masai, L.A.Vainshtein and A.S.Shlyapzeva,
Excitation Collision Strengths, Cross Sections and Rate Coefficients for OV, SiXI, FeXXIII, MoXXXIX by Electron Impact ($1s^22s^2$-$1s^22s2p$-$1s^22p^2$ Transitions) Dec.1990

NIFS-DATA-9 T.Kaneko,
Partial and Total Electronic Stopping Cross Sections of Atoms and Solids for Protons; Dec. 1990

NIFS-DATA-10 K.Shima, N.Kuno, M.Yamanouchi and H.Tawara,
Equilibrium Charge Fraction of Ions of Z=4-92 (0.02-6 MeV/u) and Z=4-20 (Up to 40 MeV/u) Emerging from a Carbon Foil; Jan.1991 [AT.Data and Nucl. Data Tables 51(1992)173]

NIFS-DATA-11 T. Kaneko, T. Nishihara, T. Taguchi, K. Nakagawa, M. Murakami, M. Hosono, S. Matsushita, K. Hayase, M.Moriya, Y.Matsukuma, K.Miura and Hiro Tawara,
Partial and Total Electronic StoppingCross Sections of Atoms for a Singly Charged Helium Ion: Part 1;Mar. 1991

NIFS-DATA-12 Hiro Tawara,
Total and Partial Cross Sections of Electron Transfer Processes for Be^{q+} *and* B^{q+} *Ions in Collisions with H,* H_2 *and He Gas Targets - Status in 1991-;* June 1991

NIFS-DATA-13 T. Kaneko, M. Nishikori, N. Yamato, T. Fukushima, T. Fujikawa, S. Fujita, K. Miki, Y. Mitsunobu, K. Yasuhara, H. Yoshida and Hiro Tawara,
Partial and Total Electronic Stopping Cross Sections of Atoms for a Singly Charged Helium Ion : Part II; Aug. 1991

NIFS-DATA-14 T. Kato, K. Masai and M. Arnaud,
Comparison of Ionization Rate Coefficients of Ions from Hydrogen through Nickel ; Sep. 1991

NIFS-DATA-15 T. Kato, Y. Itikawa and K. Sakimoto,
Compilation of Excitation Cross Sections for He Atoms by Electron Impact; Mar. 1992

NIFS-DATA-16 T. Fujimoto, F. Koike, K. Sakimoto, R. Okasaka, K. Kawasaki, K. Takiyama, T. Oda and T. Kato,
Atomic Processes Relevant to Polarization Plasma Spectroscopy ; Apr. 1992

NIFS-DATA-17 H. Tawara,
Electron Stripping Cross Sections for Light Impurity Ions in Colliding with Atomic Hydrogens Relevant to Fusion Research; Apr. 1992

NIFS-DATA-18 T. Kato,
Electron Impact Excitation Cross Sections and Effective Collision Strengths of N Atom and N-Like Ions -A Review of Available Data and Recommendations- ; Sep. 1992

NIFS-DATA-19 Hiro Tawara,
Atomic and Molecular Data for H_2O, CO & CO_2 *Relevant to Edge Plasma Impurities*, Oct. 1992

NIFS-DATA-20 Hiro. Tawara,
Bibliography on Electron Transfer Processes in Ion-Ion/Atom/Molecule Collisions -Updated 1993-; Apr. 1993

NIFS-DATA-21 J. Dubau and T. Kato,
Dielectronic Recombination Rate Coefficients to the Excited States of C I from C II; Aug. 1994

NIFS-DATA-22 T. Kawamura, T. Ono, Y. Yamamura,
Simulation Calculations of Physical Sputtering and Reflection Coefficient of Plasma-Irradiated Carbon Surface; Aug. 1994

NIFS-DATA-23 Y. Yamamura and H. Tawara,
Energy Dependence of Ion-Induced Sputtering Yields from Monoatomic Solids at Normal Incidence; Mar. 1995

NIFS-DATA-24 T. Kato, U. Safronova, A. Shlyaptseva, M. Cornille, J. Dubau,
Comparison of the Satellite Lines of H-like and He-like Spectra; Apr. 1995

NIFS-DATA-25 H. Tawara,
Roles of Atomic and Molecular Processes in Fusion Plasma Researches - from the cradle (plasma production) to the grave (after-burning) -; May 1995

NIFS-DATA-26 N. Toshima and H. Tawara
Excitation, Ionization, and Electron Capture Cross Sections of Atomic Hydrogen in Collisions with Multiply Charged Ions; July 1995

NIFS-DATA-27 V.P. Shevelko, H. Tawara and E.Salzborn,
Multiple-Ionization Cross Sections of Atoms and Positive Ions by Electron Impact; July 1995

NIFS-DATA-28 V.P. Shevelko and H. Tawara,
Cross Sections for Electron-Impact Induced Transitions Between Excited States in He: n, n'=2,3 and 4; Aug. 1995

NIFS-DATA-29 U.I. Safronova, M.S. Safronova and T. Kato,
Cross Sections and Rate Coefficients for Excitation of $\Delta n = 1$ Transitions in Li-like Ions with $6<Z<42$; Sep. 1995

NIFS-DATA-30 T. Nishikawa, T. Kawachi, K. Nishihara and T. Fujimoto,
Recommended Atomic Data for Collisional-Radiative Model of Li-like Ions and Gain Calculation for Li-like Al Ions in the Recombining Plasma; Sep. 1995